The paper proposed by C.L. Jakobs and colleagues addresses a very important subject that has received little attention for the Antarctic. It aims at demonstrating that snowmelt-albedo feedback is crucial to explain melt dynamics in the coastal Antarctic, which is expected but has never been demonstrated and quantified yet. For this, the paper uses a high-quality and long-term dataset of meteorological conditions from Neumayer station. The dataset is rich enough to allow investigating the surface energy budget in detail and the process underlying the snowmelt-albedo feedback. It is also very long for Antarctic standard (24 years) providing information on long-term changes, with an interesting climate perspective.
We thank the referee for his kind words. We will comment on each remark below. Text shown here in green has been added to the manuscript.

The paper is however difficult to read because of the structure, or maybe because some key sentences are missing. The English and style are in contrast excellent. The detailed comments below explain the issues. It is worth noting that they were written while reading the paper for the first time. I decided to keep them as is, despite the fact that some critically missing points were clarified further in the paper. Considering that most readers will read the paper from beginning to end, I think that the order of the comments is helpful to understand the necessary changes. I am optimistic that the authors will solve most of the problems by restructuring the paper and providing the key information early in the paper.
We believe that this confusion has mainly arisen from the incorrect suggestion that the albedo parameterisation is used throughout the manuscript rather than only in Sect. 4. This is now mentioned explicitly at multiple locations, which should hopefully improve the structure of the manuscript.

Another issue is the lack of robustness of the results on the feedback with respect to the methodological choices. There are a few questions and suggestions to improve this aspect below, but as a general matter, the paper should be improved by including more comparisons (with results from the literature) and with a proper discussion section putting the results in perspective with respect to other studies having the same aim, but from different regions. Melting snow in the coastal Antarctic is not so different from snow melting in other regions. This should help to consolidate the findings. Given the great potential of the paper, I encourage the authors to undertake the improvements suggested in the following.
We have added comparisons with several studies, focussing on melt climate at Neumayer, grain sizes and the snowmelt-albedo feedback. This is addressed in Sects. 3.4, 4.1 and 4.2.
[3.4]
The findings presented in this section are in good agreement with Van den Broeke et al. (2010), who used a similar approach to calculate the SEB at Neumayer, but used a lower value for $z_{0,m} = 0.32\,\mathrm{mm}$ and a higher snow density that was assumed constant with depth (420 $\mathrm{kg\,m^{-3}}$ cf. 320 $\mathrm{kg\,m^{-3}}$). Compared to melt estimates from Larsen C ice shelf, obtained through a similar modelling approach by Kuipers Munneke et al. (2012), melt at Neumayer is weak. Owing to its more northerly location, on Larsen C ice shelf an annual (2009–2011) average melt energy of $2.8\,\mathrm{W\,m^{-2}}$ is obtained, compared to the 2009–2011 annual average of $0.7\,\mathrm{W\,m^{-2}}$ obtained at Neumayer; furthermore, in November and February melt occurs much more frequently on Larsen C ice shelf.

[4.1]
Libois et al. (2015) and Picard et al. (2016) present observations of snow grain sizes on the Antarctic

plateau during field campaigns in 2012–13 and 2013–14 as well as estimates from satellite observations. On the plateau, summer temperatures are comparable to Neumayer winter temperatures. Libois et al. (2015) report summertime snow grain size estimates of approximately 0.11 mm (Fig. 6 in their study, reported as a specific surface area SSA $= \frac{3}{\rho_i r_e}$, where ρ_i is the density of ice and r_e is the snow grain size). In our study, wintertime snow grain sizes approach 0.21 mm. The difference is expected as the plateau is generally much colder than Neumayer. The seasonal cycle of modelled average snow grain size in the upper 7 cm (Fig. 8) is comparable to the one presented in Libois et al. (2015).

[4.2]
Only few studies report on the snowmelt-albedo feedback concerning the darkening of snow rather than disappearance of it. Box et al. (2012) provide relationships between anomalies of seasonal T_{2m} and SW_{net} (Fig. 5 and 12 of Box et al. (2012)). They find a negative relationship for accumulation regions, i.e. lower 2 m temperatures are associated with smaller SW_{net}. No such relationship is found for Neumayer (not shown).

Detailed comments
Abstract: the information about the accumulation is missing to my point of view, in order to put in perspective the 46mm w.e., even though there is no direct link for the very specific objective of the study.
We have added to the abstract:
This is a small value compared to an annual average (1992–2016) accumulation of 415 ± 86 mm w.e.

In my opinion, using kg/m2 for precipitation and melt is more correct and less confusing than mm w.e.
To avoid confusion, we have added the following sentence:
Throughout this paper, melt and accumulation amounts are expressed in terms of mm water equivalent (mm w.e.), which equals kg m^{-2}.

P2 L13: "Larger snow grains enhance forward scattering of photons". This is a bit incorrect, as it mixes two perspectives (radiative transfer and photon propagation). I would say "Larger snow grains has reduced scattering relative to absorption" for a pure RT perspective, or "Larger snow grains reduce backward scattering of photons" for a purely photon propagation perspective. This is a detail.
Changed
Larger snow grains reduce backward scattering of photons.

P3L10: The thickness of the top layer is very high, and I suspect that the power of the snowmelt feedback is highly sensitive to this thickness in the range 1-10mm. Skin temperature can also be very different from temperature in the uppermost 4 cm. Using small layers adds complexity which may be inadequate for regional climate modeling, but the scope of the paper is local and process oriented. It is interesting to assess in such conditions how sensitive is the investigated effect to the numerical layer thickness. Tests should be performed to show how robust the results an conclusion are to the thickness of the uppermost layers.
Thank you for this valuable suggestion. We have assessed the impact of snow layer thickness by performing a run with decreased layer thickness, i.e. 1 cm for the top layer instead of 4 cm. Although the simulation without albedo parameterisation showed only a small ($< 1\%$) increase in cumulative

amount of melt, 1154 vs. 1145 mm w.e., we decided to base the reviewed manuscript on the values obtained with the high resolution runs, as we agree that the higher resolution allows for a more accurate calculation of the snow grain size in the upper parts of the snowpack.

P3L20-25: This simplification is surprising for a study on snowmelt albedo feedback. The effect of the penetration is precisely maximum in the case of coarse/melt grains as the greater absorption is due to a deeper penetration. This seems to me a too extreme simplification given the topic of the paper and past work in this research group. At the minimum this should be assessed, somehow, by a sensitivity analysis. This is also related to the previous comment on numerical layer thickness. The argument about temperature measurement is weak, as measuring temperature in the first centimeters is anyway nearly impossible and secondly because the effect of the penetration (solid greenhouse effect) can be visible in temperature at depth when high quality surface temperature/meteorological conditions are available, as it is the case here.
Our initial motivation to neglect shortwave radiation penetration was that we assumed this effect to be small for small-grained Antarctic snow, and that our future aim is to compare SMAF with model results, in which radiation penetration is not yet considered. We however agree with the reviewer that this assumption must be assessed more completely. To take penetration of shortwave radiation into account, we implemented the relatively simple model based on 118 wavelength bands also used by Kuipers Munneke et al. (2009) (doi:10.5194/tc-3-155-2009). It is based on Brandt and Warren (1993) (doi:10.3198/1993JoG39-131-99-110), who used the two-stream model by Schlatter (1972) (doi:10.1175/1520-0450(1972)011<1048:TLSEBA>2.0.CO;2). In this model, the amount of absorbed shortwave radiation amongst other things depends on layer density and layer grain size, which are provided in look-up tables for seven different snow grain sizes, which we interpolate to the grain sizes obtained from the albedo parameterisation.

A melt increase of 13% is found when radiation penetration is included: 1326 mm w.e. compared to 1154 mm w.e., but average SMAF did not change. We thus conclude that including penetration of shortwave radiation using a simple radiation transport model does increase the amount of modelled melt in an absolute sense, but that the SMAF results are robust to both the layer thickness and whether or not shortwave radiation penetration is included. We now include a discussion on the effect of shortwave radiation penetration (see below), and included the effect in the SMAF uncertainty estimate in Fig. 14.
[2.1]
Subsurface penetration of shortwave radiation is calculated using a spectral model (Kuipers Munneke et al., 2009), based on the parameterisation by Brandt and Warren (1993), which is in turn based on the two-stream radiation model of Schlatter (1972). The impact on modelled melt and the quantification of the snowmelt-albedo feedback is discussed in the relevant sections.

[3.3]
Using the subsurface radiation model of Kuipers Munneke et al. (2009), the influence of subsurface penetration of shortwave radiation is estimated. Its inclusion increases the cumulative amount of melt by 13 %, from 1154 mm w.e. to 1326 mm w.e. The absorbed shortwave radiation heats the subsurface layers, but the heat cannot be transported away as effectively as would happen at the surface by turbulent fluxes and longwave radiation. This leads to an increase in total melt.

[4.2]
The effect of subsurface penetration of shortwave radiation on this result is estimated by repeating

the above experiments with inclusion of the radiation penetration model of Kuipers Munneke et al. (2009). This yielded an average SMAF of 2.3, ranging from 1.5 (2005–06) to 3.2 (2002–03). The main difference between the two experiments is the reduced interannual variability: including penetration of shortwave radiation does not yield SMAF values larger than 3.5. Shortwave radiation penetration heats the subsurface, causing subsurface melt which is less affected by the snowmelt-albedo feedback because the radiative flux is smaller in the subsurface. Therefore, the 'extreme' years in the sense of SMAF are less distinct in the experiment with shortwave radiation penetration. The effect of shortwave radiation penetration is included in the uncertainties indicated in Fig. 10c. Combining this with the uncertainties in observed $SW\uparrow$ and the determination of τ (Fig. 2b) leads to uncertainties in the determination of the SMAF of typically 15 %, with a range of 4 % (1995–96) to 32 % (1993–94).

P3L30: I would remove the emissivity symbol because this equation is only complete for emissivity of 1 (as assumed here). A more correct equation is LWup = sigma eps Tsˆ4 + (1-eps) LWdown. This significantly reduces the sensitivity to eps (as much as the sky is covered by low clouds) compared to the incomplete equation, so would avoid the first part of the comment in P6L26.
The model is able to work with an emissivity different from 1 and in that case it will employ the correct equation. As in this study $\epsilon = 1$, it is not necessary to write it in the equation. We have now clarified this.
(...)using Stefan-Boltzmann's law for a longwave emissivity $\epsilon = 1$:

$$LW\uparrow = \sigma T_s^4, \tag{2}$$

P4L5: The approach is surprising, as explained and justified, but I guess this results from an unsuccessful attempt to, conventionally, use SWdown ? If not, this should obviously be tested. If yes, a more direct explanation of what has been done should be presented with some developments. In particular, a detection and statistical study of riming would be interesting, if this is an important problem to collect the data, in particular on how it correlates with melt (I intuitively expect a negative correlation). This section is confusing.
The choice to use measured $SW\uparrow$ instead of measured $SW\downarrow$ (and 'calculating' $SW\downarrow$) is motivated by findings by e.g. Van den Broeke et al. (2004) and Smeets et al. (2018) who showed that the upward-facing sensor (which measures an important direct radiation component) is more prone to inaccuracies due to tilt and riming. The simulations with the observed albedo use $SW\uparrow$ combined with the 24-hour running mean albedo to construct $SW\downarrow$ and SW_{net}. Using a running mean albedo instead of the instantaneous observed albedo further reduces measurement errors due to tilt and riming. The simulations with parameterised albedo use $SW\uparrow$ combined with the parameterised albedo to obtain $SW\downarrow$ and SW_{net}. We now cite the paper in which this method is explained (Van den Broeke et al., 2004), and added to the manuscript:
Because the shortwave radiation sensor faces the sky and includes a significant direct component, measured $SW\downarrow$ suffers from relatively large uncertainties owing to poor sensor cosine response, sensor tilt and/or rime formation (Smeets et al., 2018). In order to improve the accuracy of observed net shortwave radiation used in the SEB calculations (Sect. 3), we calculate SW_{net} based on $SW\uparrow$, which is diffuse and hence much less sensitive to these errors, in combination with a 24-hour moving average albedo, as described in Van den Broeke et al. (2004). In Sect. 4, in which albedo is parameterised to study melt-albedo feedbacks, for consistency we use measured $SW\uparrow$ in combination with parameterised albedo to estimate SW_{net}.

P4L20: Since grain growth is very sensitive to liquid water content (cubic power) which comes from the melted mass (constrained by available energy) and the layer thickness, this growth is thus very sensitivity to layer thickness (inverse of cubic power?). Here again I suggest to perform a sensitivity to the numerical layer thickness. Exploring the range 1-5cm should be adequate for this aspect, to stay far from divergence at very small layer thicknesses. I'm afraid this sensitivity analysis could greatly affect the result section... and change the paper.
The effect of upper layer thickness was addressed in the response to the comment on P3L10. Only small differences were found, and the current values in the manuscript are obtained from simulations with a smaller layer thickness (1 cm).

Figure 2: make the individual dots partially transparent (alpha parameter) to better represent the density of dots (or make the dots smaller but the effect is usually better with transparency). The actual representation can be misleading when the number of dots is huge (the case here) and the density is uneven.
Good suggestion, we have changed the figures accordingly.

Figure 3: The title seems incorrect. Is it right that a sensitivity analysis has been done using a Monte-Carlo approach (chose random pair of z0 and density, run the model and compute RMSE) ? If yes, the graph does not show the relationship between these two parameters, but instead the RMSE and bias as function of both parameters. Still if I understand well, I suggest as a small improvement (for a next paper) to use quasi-random generator instead of pseudo-random. A Voronoi interpolation would also improve the graph. This is not critical.
Yes, a Monte-Carlo approach was used for this sensitivity analysis. However, we decided to remove Fig. 3 as it is not important for the final experiments and conclusions.

P6L19-20: This sentence is hard to follow without the formulations. Equations could be added in the method section.
We have added the relevant formulations in the methods section.
Surface roughness lengths for momentum, heat and moisture are related through the expression of Andreas (1987):

$$\ln\left(\frac{z_{0*}}{z_{0,m}}\right) = a_1 + a_2 \ln\left(\mathrm{Re}_*\right) + a_3 \ln\left(\mathrm{Re}_*\right)^2 , \tag{3}$$

where z_{0*} represents either $z_{0,h}$ or $z_{0,q}$, the roughness lengths for heat and moisture respectively, a_1, a_2 and a_3 are coefficients determined by Andreas (1987) for various regimes of the roughness Reynolds number $\mathrm{Re}_* = \frac{u_* z_{0,m}}{\nu}$ with kinematic viscosity ν and friction velocity u_*.

Figure 4: I again suggest transparency on dots + remove non significant numbers for R2, bias and RMSE (same for Fig 12).
We have changed the figure, removed the digits.

P6L25: Maybe. It could also be a problem of calibration of the radiometer. In such case all the Ts,obs would be scaled down. I suggest to 1) show transparent dots to visualize if these cases are frequent or not, and 2) check that Ts>273.15K occurs mainly for low wind to support the proposed hypothesis of heating. Otherwise, consider to 'recalibrate' the radiometer by scaling down its efficiency to reduce the number of Ts over 273.15K. It may be necessary to use the complete LWup and emissivity close to 0.98 to make this test. Recalibration may lead to a significant effect on snowmelt simulations.

Measured $T_s > 273.15$ K values were only present in the first couple of years, afterwards they were removed through post-processing by AWI. $T_S > 273.15$ K indeed occurred mostly when wind speed was relatively low (potentially causing heating of sensor window). Furthermore, measurements of $T_s > 273.15$ K could be a result of the radiation sensor partly measuring longwave radiation emitted by the air between the surface and the sensor at 2 metre height, but we deem this less likely in this cold environment. We added to the manuscript:
Measured values of T_s in excess of the melting point in Fig. 4 only occurred in the first 6 seasons; from 1998–99 onwards they were removed by additional post-processing. These measurements mainly reflect uncertainties in the adopted unit value of longwave emissivity and in measured $LW\uparrow$, e.g. from sensor window heating (Smeets et al., 2018) and the fact that the downward facing radiation sensor also measures longwave radiation emitted by the relatively warm air between the surface and the sensor.

Figure 5: This figure is a bit complex to read despite its apparent simplicity, I have spent some time to understand why the steps and what is the black/red mixture. I suggest to show the grid (vertical dotted gray line on 1st Jan of each year or another way to visualize the summers). The "shaded red area" appears as a line, it would be better to remove it. The necessary info is in the text and is also next to the discussion P6L30-34 which is very good and give a more correct impression of the potential uncertainties than the red area. I'm also wondering about the interest of showing (only) the cumulative melt. I have spent some time to mentally derivate the curve to see the temporal trend and variability (then I realize later it is in Fig 8...). I suggest to add a plot with annual melt along with the cumulative time-series. The measurement error might be more visible on this plot.
We have added grey patches from 1 Nov–1 Mar to help the reader in finding the melt seasons. The shaded red area indeed is very narrow, owing to the small uncertainty due to the measurement errors, so we have removed it. We have added a second plot with seasonal melt amounts, also without the uncertainty due to measurement errors as it was barely visible anyway. We changed the caption accordingly:
Effect of model uncertainties on **(a)** cumulative melt and **(b)** seasonal melt. The shaded area indicates the 1σ range due to model uncertainties (changing $z_{0,m}$ and $\rho_{s,0}$ between their respective values) which is asymmetrical because the values that are used for the rest of the study ($z_{0,m} = 1.65\,\mathrm{mm}$, $\rho_{s,0} = 280\,\mathrm{kg\,m^{-3}}$) are not in the middle of the range that was probed. The vertical grey patches in **(a)** indicate Nov–Feb of each year. Note that **(b)** ends earlier than **(a)** because the observations do not cover the 2015–16 melt season entirely.

Section 3.2. It is relatively disconnected from the remaining. This could be moved to the data section, or at least before Section 3.1
We have moved the discussion about the local climate to Sect. 2.3.1.

Figure 7: the color is not visible. Is it possible to make wind roses (showing wind speed and direction as e.g. in Champollion et al. 2013 in TC) for 2 or 3 classes of T2m-Ts (e.g. <5 and >5) ? In the end, is the information on temperature so useful ?
We agree that the discussion about wind direction and wind speed does not contribute to the paper final discussion and conclusions. We have therefore removed this figure.

P7L19: Is it relative to water or ice ? Relative to ice is more relevant over the ice-sheet.
The conversion from specific humidity to relative humidity takes the present air temperature into account. Depending on the prevailing air temperature, the saturated vapour pressure with respect

to either water or ice is used. We added:
(relative to either water or ice, depending on the air temperature)

P7L29: I don't see in Fig 8 and Table 2 that SEB is dominated by SWnet. What does this mean ? All the plots in Figure 8 have a different y-axis scaling, which makes difficult to judge the dominance of one or another terms.
The reference should have been Fig. 6b (now Fig. 3b), which presents the seasonal cycle of the SEB components, and, as we should have stressed, *in summer*. This has now been corrected
Annual (Mar–Feb) mean values of near-surface meteorological quantities and SEB components are presented in Table 2, with seasonal cycles of SEB components presented in Fig. 3b. These show that the summertime SEB is dominated by the radiation fluxes...

P8L6: Ts could be shown in Fig 8 (along with Tair).
We have removed the panel with the timeseries as we think they do not contribute to the overall goal of the study.

P8L27: "The difference in SWnet is caused solely by surface albedo". How to exclude the cloudiness as a cause ? Has the LWdown changed between the two years ? More generally how does this interact with the 'unconventional' approach use to compute the SW fluxes. Is it mainly an observational results or an intrinsic consequence of the model and approach ? On a one hand I'm impressed that SW down is equal for both years suggesting that the model predicts the right grain size that perfectly remove the albedo dependence from SWup. However a constant SWdown between both years is only expected if cloudiness has not changed. It is worth checking this, because this is an indirect validation of the approach and of the model grain size.

From the original manuscript it was unclear that these simulations have been performed with the observed albedo instead of the parameterised albedo. Therefore, there is no 'prediction' for grain size by the model in this figure. We have included more components in Fig. 10 to show that both $SW\downarrow$ and $LW\downarrow$ do not differ between these years. Therefore, we conclude that the difference in SW_{net} comes from $SW\uparrow$, driven by changes in surface albedo. In response, $LW\uparrow$ changes as the surface is warmer in high melt years, leading to the change in LW_{net}. We added to the manuscript:
$SW\downarrow$ and $LW\downarrow$ show almost no difference between high and low melt seasons; therefore, the difference in SW_{net} cannot be caused by a change in cloud cover and is likely caused solely by surface albedo...

P9L6: Picard et al. 2012 (doi:10.1038/nclimate1590) may be a useful citation at this point.
We have added this citation.
Precipitation of new, fine-grained snow has been shown to inhibit the albedo decrease by metamorphism on the Antarctic plateau (Picard et al., 2012).

P9L17: It is not clear in the data section that SWdown was not excluded (due to riming) and used to compute observe albedo. This Section 4.1 should be moved in the Method section, because it is necessary to understand the previous section results (see my comment P8L27).
Thank you for your suggestion. This is achieved by restructuring and adding sentences to clarify the difference between the simulations for Sects. 3 and 4 (see response to second comment).

P9L25: Picard et al. 2012, Libois et al. 2015 and Picard et al. 2016 provide observed relationship

between dry snow albedo and grain size.
We have added a comparison of snow grain sizes in the manuscript, as mentioned in the response to the third general comment.
Libois et al. (2015) and Picard et al. (2016) present observations of snow grain sizes on the Antarctic plateau during field campaigns in 2012–13 and 2013–14 as well as estimates from satellite observations. On the plateau, summer temperatures are comparable to Neumayer winter temperatures. Libois et al. (2015) report summertime snow grain size estimates of approximately 0.11 mm (Fig. 6 in their study, reported as a specific surface area SSA $= \frac{3}{\rho_i r_e}$, where ρ_i is the density of ice and r_e is the snow grain size). In our study, wintertime snow grain sizes approach 0.21 mm. The difference is expected as the plateau is generally much colder than Neumayer. The seasonal cycle of modelled average snow grain size in the upper 7 cm (Fig. 8) is comparable to the one presented in Libois et al. (2015).

P9L27: "to best match the cumulative melt using observed albedo.". I do not understand what has been done. It seems in contradiction with Section 2.2 which indicates that SWdown is not used because unreliable. How to compute valid albedo in these conditions ? In any case this kind of information is required in the method section before the result section Additionally, it seems relevant to show the observed albedo evolution if it exists.
By explicitly stating that the observed albedo was used in Sect. 3 we believe it is now clear what has been done to have the simulation with parameterised albedo adequately reproduce the cumulative melt of the simulation with observed albedo.

P10L5: CNR4 are given for SZA>60.
At Neumayer, not the rather simple CNR4-net radiometer was used but more sophisticated pyranometers. In 1992 the AWI started using artificially ventilated K&Z CM11 instruments and in 2009 switched to the even better K&Z CM22. Both have a much better cosine response compared to the CNR4. The cosine error for solar zenith angles greater than 60 degrees for the used pyranometers is part of the measurement errors listed in Table 1.

P10L19-20: are these metrics calculated over the summer or the year ?
Only summer values are used for these metrics.
A weak positive correlation was found between SMAF and $SW\downarrow$ ($R^2 = 0.15,\ p = 0.07$); if $SW\downarrow$ increases, more energy is available at the surface for melting, which is then in turn further intensified by SMAF. Another weak negative correlation was found between SMAF and summer precipitation ($R^2 = 0.13,\ p = 0.09$); snowfall inhibits SMAF as it effectively 'resets' the surface albedo as was also shown by Picard et al. (2012).

Section 4.2: From here, I start to understand what I have missed before. It is not clear that the main simulation was done with measurements of SWdown and SWup because the Section 2.2 emphasizes the unconventional approach and the albedo parameterization. I let the previous comments written before reaching this section because they highlight the problem for who reads the paper linearly Nevertheless, I'm still concerned by the interaction between the approach and the finding of the importance of the snowmelt-albedo feedback. The results seem to entirely rely on the calibration of the metamorphism and albedo parameterizations and their validation is to limited. For instance, over-estimating grain growth in wet conditions automatically leads to over-estimate the importance of SMAF. Ideally, comparison with data from the literature (even on seasonal snow, which is subject to comparable conditions when melting) would help to consolidate a little bit more the result. I

was also expecting a discussion section comparing SMAF with the literature.
As mentioned in response to the third general comment, we changed the structure of the paper and added sentences in such a way that it is now more clear what has been done to obtain the optimal settings for grain size calculation and the associated parameterised albedo. Furthermore, we included comparisons with several other studies, in Sects. 3.4, 4.1 and 4.2.

The discussion at the end of P10 confirms the lack of robustness. The sensitivity to the numerical layer thickness which I propose before is likely to further weaken the findings of this section.
We now included several comparisons with literature, as mentioned in the response to the third comment. We also now more clearly emphasise the use of observed albedo in Sect. 3 and the parameterised albedo in Sect. 4, such that it is immediately clear that the results presented in Sect. 3 do not rely on the albedo parameterisation.

A possible solution is to define SMAF from R0 and R1', where R1' uses the albedo at the end of the winter (and not the annual average of albedo). This would avoid to rely on the grain growth and grain-albedo parameterization, and would be more robust. At least, it should be checked that R1' is close and lower than R3. The main drawback of using R1' is neglecting the dependency on cosine(SZA) which tends to reduce albedo and increase melt during the summer, in parallel with the grain growth.
The average albedo at the end of the winter (taken as the first day that the Sun rises above 10° altitude, and then take the preceding 48-hour mean albedo) is 0.87 (cf. the full period average albedo of 0.84). Prescribing this albedo throughout the run yields a cumulative amount of melt of 460 mm w.e., and subsequently a SMAF of 2.5 (slightly higher than the high resolution run, which yielded a SMAF of 2.4). The total amount of melt in the R_1' run is slightly higher than that was modelled by R_3 (which totalled 428 mm w.e.). The variability in SMAF according to R_1' is much larger than the one calculated by R_3 and sometimes becomes less than one, which is unphysical. As pointed out by the referee, using this measure neglects the dependency on the zenith angle and the impact of precipitation or the periods between precipitation events during the summer season. Therefore, we decided to keep the original definition of SMAF in the manuscript. We have added: Alternatively, SMAF could be defined as the ratio between R_0 and R_3, or the ratio between R_0 and R_1', where R_1' uses the average albedo at the end of the winter. Using the former definition, the results become more prone to noise due to the performance of the albedo parameterisation itself. The latter definition neglects the dependency on solar zenith angle and the impact of precipitation. Therefore, we believe defining SMAF as the ratio between R_2 and R_3 is more consistent.

The manuscript "Quantifying the snowmelt-albedo feedback at Neumayer Station, East Antarctica" by Jacobs et al. presents meteorological data and simulation results to determine the albedo feedback effect at a single point for an ice shelf region of Antarctica. The chosen location (Neumayer Station) is well-equipped with instruments to measure four component radiation and sensors are maintained regularly. Such data allow for determination of contributing parameters such as surface roughness and microscale wind fields to estimate full energy balance. I consider the quantification of the melt albedo feedback as highly relevant for the cryospheric community especially for snow on ice sheets. However, some missing information as well as the confusing structure of the manuscript prevent publication in the current state.
We thank the referee for their constructive comments. They are addressed below in a structured way. Text in green shows text as it is now in the manuscript.

Major points of criticism are:

- The reader gets very confused by the structure of the manuscript. I recommend to revise carefully. The presented results sections consist of results and discussion, while large fractions of the first results (Section 3) mostly consist of data presentation. In addition, measured data and results simulated by model approaches are constantly mixed in Figures and text. It would be much easier to follow if measured parameters such as temperature, wind, humidity and radiation are separated from generated parameters such as Q_s, Q_l etc.
Thank you for this suggestion. We have separated the presentation of the local near-surface climate from the discussion of the surface energy balance. The near-surface climate discussion is moved to Sect. 2.

Same appears for manuscript sections and paragraphs: for instance, P6 L12-20 is solely discussion same as P6 L29-L3 P7 while before and after those paragraphs you mix measured data and model outputs.
We have moved blocks of text in Sect. 3.2 in order to present and discuss the results in a more logical manner.

In addition, the manuscript title indicates quantification of the melt albedo feedback, while only 2 pages and 2-3 Figures (out of 13 – not mentioning the numerous panels) are referring to snowmelt and albedo feedbacks. I understand that it is necessary to introduce the meteorological data, however, please carefully evaluate the necessity of the presentation of each parameter (Figs 6-9) with sometimes redundancies in the text. Some of the Figures would fit into a supplementary material section. I consider the colorbar in Fig. 7 as being useless. It is impossible to identify differences.
We have removed Figs. 3, 7, 8 and 11 to enhance readability.

- The nomenclature is sometimes not correct. First of all, what is "fresh snow"? I assume you refer to new snow, which would not be the correct nomenclature either. New snow refers to "Recently fallen snow in which the original form of the ice crystals can be recognized" among others presented in Fierz et al. (2009). The term recently implies a defined time frame. The snow you refer to in the manuscript can rather be defined as near surface snow or surface snow for which you should define a depth range as well. Such a surface snow undergoes rapid transformations especially for polar regions on ice sheets.
With fresh snow we refer to new snow as defined by Fierz et al. (2009). The contribution of "fresh

snow" as it is in the albedo parameterisation solely comes from recently fallen snow in a defined time frame, namely the timestep of the model. Snow that was already present in the layer from the previous timestep is considered "old snow", which undergoes the dry snow metamorphism. We have now made this more clear in the manuscript by changing "fresh snow" to "new snow" throughout the manuscript.

I am not sure I understand which formulations are used to estimate snow metamorphism at the surface. It might be beyond the scope of the manuscript but you should distinguish between temperature gradient metamorphism (TGM), equi-temperature metamorphism, melt-freeze metamorphism and Firnification and pressure metamorphism. The latter two can be excluded for surface snow but simply assuming grain growth by melt-freeze metamorphism has to be discussed more in detail. Can you present in-situ data on surface densities and grains recorded by the staff at Neumayer? Please see the following paper for more details on metamorphism (Calonne et al. 2014;doi:10.5194/tc-8-2255-2014). Grain size might be a good tuning parameter but is not a parameter quantifying adequately properties of snow. For the here referred optical properties, it is recommended to use the optical-equivalent grain size or specific surface area (SSA). Again, this might be beyond the scope of the paper but you should at least be up to date with nomenclature and references.
We have added the formulation of dry snow metamorphism. Unfortunately, no in-situ data on surface densities or grains are available from Neumayer. We have now included a comparison with measurements on the Antarctic Plateau (Picard et al. 2012; doi:10.1038/nclimate1590). Although the local climates are very different, the comparison shows that the grain sizes measured on the plateau in summer are similar to the grain sizes modelled at Neumayer in winter. Neumayer winter temperatures are somewhat comparable to plateau summer temperature. We added to the manuscript:
[2.2]
Dry snow metamorphism is parameterised following Kuipers Munneke et al. (2011b):

$$\frac{\mathrm{d}r_{e,dry}}{\mathrm{d}t} = \left(\frac{\mathrm{d}r_e}{\mathrm{d}t}\right)_0 \left(\frac{\eta}{(r_e - r_{e,0}) + \eta}\right)^{1/\kappa}, \tag{9}$$

where $r_{e,0}$ is the new snow grain size, and the coefficients $\left(\frac{\mathrm{d}r_e}{\mathrm{d}t}\right)_0$, η and κ are obtained from a look-up table. This look-up table is compiled based on simulations with the SNICAR model (Flanner et al., 2006), which calculates the snow metamorphism resulting from temperature gradient metamorhpism.

[4.1]
Libois et al. (2015) and Picard et al. (2016) present observations of snow grain sizes on the Antarctic plateau during field campaigns in 2012–13 and 2013–14 as well as estimates from satellite observations. On the plateau, summer temperatures are comparable to Neumayer winter temperatures. Libois et al. (2015) report summertime snow grain size estimates of approximately 0.11 mm (Fig. 6 in their study, reported as a specific surface area SSA $= \frac{3}{\rho_i r_e}$, where ρ_i is the density of ice and r_e is the snow grain size). In our study, wintertime snow grain sizes approach 0.21 mm. The difference is expected as the plateau is generally much colder than Neumayer. The seasonal cycle of modelled average snow grain size in the upper 7 cm (Fig. 8) is comparable to the one presented in Libois et al. (2015).

- Please quantify parameterizations (e.g. P9 L16-17).

We have added the ranges that were probed for the new snow and refrozen snow grain sizes. These parameters were varied within reasonable ranges to optimise the results: new snow grain size between 0.04 mm and 0.3 mm, refrozen snow grain size between 0.1 mm and 10 mm.

- Please be consistent: snow pack versus snowpack. I recommend to use snowpack as stated in Fierz et al. 2009. Same appears for T_s as surface temperature or T_0 as in Fig. 7 or P3 L10.
We have changed snow pack to snowpack throughout the manuscript. T_0 on P3 L10 should have been a T_s.

Quantifying the snowmelt-albedo feedback at Neumayer Station, East Antarctica

Constantijn L. Jakobs[1], Carleen H. Reijmer[1], Peter Kuipers Munneke[1], Gert König-Langlo[2], and Michiel R. van den Broeke[1]

[1]Institute for Marine and Atmospheric Research Utrecht, Utrecht University, Utrecht, The Netherlands
[2]Alfred-Wegener-Institut Helmholtz-Zentrum für Polar- und Meeresforschung, Bremerhaven, Germany

Correspondence: Stan Jakobs (c.l.jakobs@uu.nl)

Abstract. We use 24 years (1992–2016) of high-quality meteorological observations at Neumayer Station, East Antarctica, to force a surface energy balance model. The modelled 24-year cumulative surface melt at Neumayer amounts to 1154 mm water equivalent (w.e.), with only a small uncertainty (± 3 mm w.e.) from random measurement errors. Results are more sensitive to the chosen value for the surface momentum roughness length and new snow density, yielding a range of 900–1220 mm w.e. Melt at Neumayer occurs only in the months November to February, with a summer average of 50 mm w.e. and large interannual variability (σ = 42 mm w.e.). This is a small value compared to an annual average (1992–2016) accumulation of 415 ± 86 mm w.e. Absorbed shortwave radiation is the dominant driver of temporal melt variability at Neumayer. To assess the importance of the snowmelt-albedo feedback we include and calibrate an albedo parameterisation in the surface energy balance model. We show that, without the snowmelt-albedo feedback, surface melt at Neumayer would be approximately three times weaker, demonstrating how important it is to correctly represent this feedback in model simulations of surface melt in Antarctica.

1 Introduction

The Antarctic ice sheet (AIS) contains more than 25 million km^3 of ice, sufficient to raise global mean sea level by almost 60 m if melted completely (Fretwell et al., 2013). Between 1992 and 2017, the AIS lost mass at an accelerated rate, contributing 7.6 ± 3.9 mm to global sea level (Shepherd et al., 2018). This mass loss is mainly observed in coastal West Antarctica and the Antarctic Peninsula (AP), and is caused by glaciers that accelerated after their buttressing ice shelves had thinned or disintegrated (Wouters et al., 2015; Turner et al., 2017). The interaction between meltwater and firn, the intermediate product between snow and glacier ice, is hypothesised to play an important role in ice shelf disintegration (Kuipers Munneke et al., 2014). If the firn layer contains enough air, as is the case for most of the AIS, meltwater can percolate downwards and refreeze (Ligtenberg et al., 2014). If the storage capacity of the firn layer is reduced, surface meltwater can flow laterally towards the ice shelf edge (Bell et al., 2017), be stored englacially (Lenaerts et al., 2017) or form ponds on the ice shelf surface (Kingslake et al., 2017). In all cases, meltwater can accumulate in crevasses, thereby increasing the hydrostatic pressure in the crevasse tip, causing it to penetrate farther down. When a crevasse reaches the bottom of the ice shelf or a basal crevasse, part

of the ice shelf disintegrates, a process called hydrofracturing (Van der Veen, 2007). Hydrofracturing has been identified as a potential precursor to rapid loss of Antarctic ice, accelerating sea level rise (DeConto and Pollard, 2016). In combination with enhanced ocean swell under low sea-ice conditions (Massom et al., 2018), hydrofracturing likely caused the disintegration of Larsen B ice shelf in the AP in 2002 (Rignot et al., 2004; Scambos et al., 2004). In July 2017, a large iceberg calved from Larsen C ice shelf, but it is unclear whether this signifies a further southward progression of ice shelf destabilisation in the AP (Hogg and Gudmundsson, 2017).

Improving our predictive capabilities of future ice shelf stability, AIS mass loss and associated sea level rise, thus requires a thorough understanding of the surface melt process on Antarctic ice shelves. In contrast to meltwater occurrence, which is readily observed from space (Picard et al., 2007; Tedesco, 2009; Luckman et al., 2014), observational estimates of surface melt *rates* on Antarctic ice shelves are rare; they have been obtained locally through explicit modelling of the surface energy balance (SEB) (Van den Broeke et al., 2010; Kuipers Munneke et al., 2012, 2018). In turn, these enabled continent-wide melt rate estimates using calibrated satellite products based on backscatter strength of radio waves (Trusel et al., 2013, 2015). These studies invariably demonstrate that in most parts of Antarctica, melt currently is a weak and intermittent process. In this melt regime, the positive snowmelt-albedo feedback plays a decisive role: when snow melts, meltwater may refreeze in the cold snowpack, resulting in considerably larger grains (~ 1 mm) than new snow or snow that has been subjected to dry compaction (~ 0.1 mm). Larger snow grains reduce backward scattering of photons into the snowpack, increasing the probability of absorption, reducing the surface albedo especially in the near-infrared (Wiscombe and Warren, 1980; Gardner and Sharp, 2010). This further enhances absorption of solar radiation and melt. For pure, uncontaminated snow, the strength of the snowmelt-albedo feedback depends on multiple factors, e.g. the intensity and duration of the melt and the frequency and intensity of snowfall events, which provide new snow consisting of smaller grains. We therefore expect the snowmelt-albedo feedback to be spatially and temporally variable on Antarctic ice shelves.

Most studies on the snowmelt-albedo feedback address the removal of (seasonal) snow and the appearance of dark soil or water (Perovich et al., 2002; Hall, 2004; Flanner et al., 2007; Qu and Hall, 2007), leading to further warming of the air/water. These studies commonly express the melt-albedo feedback in terms of air/water temperature sensitivity. Our aim is to quantify the impact on the melt rate of the darkening but not the disappearance of snow, a process addressed by far fewer studies (Box et al., 2012; Van As et al., 2013). To that end, we implement a snow albedo parameterization (Gardner and Sharp, 2010; Kuipers Munneke et al., 2011b) in an SEB model, which is then calibrated using observations and used to study the sensitivity of melt rates to snow properties that influence snow albedo. We use 24 years of high-quality in situ observations (König-Langlo, 2017) from the German research station Neumayer (Fig. 1) to calculate the SEB and melt rate. We investigate the effects of measurement uncertainties and model settings on the calculated cumulative amount of surface melt. We then analyse the main drivers of surface melt and the magnitude of the snowmelt-albedo feedback at Neumayer by switching on/off the feedback process in the albedo parameterisation.

The SEB model is explained in Sect. 2.1, followed by a description of the albedo parameterisation in Sect. 2.2. The meteorological data used to force the SEB model are described in Sect. 2.3. The results section is split into two parts; in Sect. 3 we

present and discuss the SEB and melt rate that are obtained using the observed albedo. In Sect. 4 the albedo parameterisation is used instead and the snowmelt-albedo feedback is quantified and discussed. Finally, the results are briefly discussed in Sect. 5.

2 Methods

2.1 Surface energy balance model

The one-dimensional energy balance model is a further development of the models presented by Reijmer et al. (1999), Reijmer and Oerlema (2002), Van den Broeke et al. (2005) and Kuipers Munneke et al. (2012); here only the main features are described. The energy balance of an infinitesimally thin surface layer (the 'skin' layer) is defined as:

$$M = SW\downarrow + SW\uparrow + LW\downarrow + LW\uparrow + Q_S + Q_L + Q_G \tag{1}$$

where positive fluxes are defined to be directed towards the surface. $SW\downarrow$ and $SW\uparrow$ are the incoming and reflected shortwave radiation, $LW\downarrow$ and $LW\uparrow$ are the downward and upward longwave radiation, Q_S and Q_L the turbulent sensible and latent heat fluxes and Q_G is the conductive subsurface heat flux. We neglect latent energy from rain. M is the energy used to melt snow or ice, and is non-zero only when the surface has reached the melting point of ice ($T_s = 273.15\,\mathrm{K}$). Throughout this paper, melt and accumulation amounts are expressed in terms of mm water equivalent (mm w.e.), which equals $\mathrm{kg\,m^{-2}}$. In order to calculate Q_G and allow for densification, meltwater percolation and refreezing, a snow/firn model is used, initialised with 70 layers. The layer thickness varies from 1 cm at the top to 2 m at the bottom (25 m depth). We impose a no-energy flux boundary condition at the lowermost model level. New snow density is parameterised following the expression of Lenaerts et al. (2012), which relates it to the prevailing surface temperature (T_s) and 10 m wind speed (V_{10m}) and imposes a lower limit of new snow density $\rho_{s,0}$. Meltwater percolation is based on the tipping-bucket method (e.g. Ligtenberg et al., 2011), allowing for immediate downward transport (within a single timestep of 10 s) of remaining water if a layer has attained its maximum capillary retention, as modelled using the expressions of Schneider and Jansson (2004). Meltwater refreezing increases the density and temperature of a layer. At the bottom of the firn layer, the meltwater is assumed to run off immediately, i.e. the model does not allow for slush/superimposed ice formation or lateral water movement. The calculation of the turbulent fluxes is based on Monin-Obukhov similarity theory between a single measurement level (2 m for temperature and humidity, 10 m for wind) and the surface, assuming the latter to be saturated with respect to ice and using the stability functions according to Dyer (1974) for unstable and Holtslag and De Bruin (1988) for stable conditions.

Subsurface penetration of shortwave radiation is calculated using a spectral model (Kuipers Munneke et al., 2009), based on the parameterisation by Brandt and Warren (1993), which is in turn based on the two-stream radiation model of Schlatter (1972). The impact on modelled melt and the quantification of the snowmelt-albedo feedback is discussed in the relevant sections.

The terms in Eq. (1) are either based on observations or can be expressed as a function of the skin temperature T_s. The SEB is solved iteratively by looking for a value of T_s that closes the SEB to within 0.005 K between iterations: if $T_s > 273.15\,\mathrm{K}$, it is reset to 273.15 K and excess energy is used for surface melt M. To evaluate model performance, the modelled value of T_s is

compared to observed T_s calculated from $LW\uparrow$, using Stefan-Boltzmann's law for a longwave emissivity $\epsilon = 1$:

$$LW\uparrow = \sigma T_s^4, \tag{2}$$

where $\sigma = 5.67 \cdot 10^{-8}\,\mathrm{W\,m^{-2}\,K^{-4}}$ is the Stefan-Boltzmann constant.

Surface roughness lengths for momentum, heat and moisture are related through the expression of Andreas (1987):

$$\ln\left(\frac{z_{0*}}{z_{0,m}}\right) = a_1 + a_2 \ln(\mathrm{Re}_*) + a_3 \ln(\mathrm{Re}_*)^2, \tag{3}$$

where z_{0*} represents either $z_{0,h}$ or $z_{0,q}$, the roughness lengths for heat and moisture respectively, a_1, a_2 and a_3 are coefficients determined by Andreas (1987) for various regimes of the roughness Reynolds number $\mathrm{Re}_* = \frac{u_* z_{0,m}}{\nu}$ with kinematic viscosity ν and friction velocity u_*.

2.2 Albedo parameterisation

Because the shortwave radiation sensor faces the sky and includes a significant direct component, measured $SW\downarrow$ suffers from relatively large uncertainties owing to poor sensor cosine response, sensor tilt and/or rime formation (Smeets et al., 2018). In order to improve the accuracy of observed net shortwave radiation used in the SEB calculations (Sect. 3), we calculate SW_{net} based on $SW\uparrow$, which is diffuse and hence much less sensitive to these errors, in combination with a 24-hour moving average albedo, as described in Van den Broeke et al. (2004). In Sect. 4, in which albedo is parameterised to study melt-albedo feedbacks, for consistency we use measured $SW\uparrow$ in combination with parameterised albedo to estimate SW_{net}.

In Sect. 4, the parameterised surface albedo α is described as a base albedo α_S, modified by perturbations describing the effect of changing solar zenith angle θ ($\mathrm{d}\alpha_u$), the cloud optical thickness τ ($\mathrm{d}\alpha_\tau$) and the concentration of black carbon in the snow ($\mathrm{d}\alpha_c$) (Gardner and Sharp, 2010; Kuipers Munneke et al., 2011b):

$$\alpha = \alpha_S + \mathrm{d}\alpha_u + \mathrm{d}\alpha_\tau + \mathrm{d}\alpha_c. \tag{4}$$

For Antarctica, we neglect the impact of impurities in the snow ($\mathrm{d}\alpha_c = 0$); $\mathrm{d}\alpha_u$ and $\mathrm{d}\alpha_\tau$ both depend on the base albedo α_S, $\mathrm{d}\alpha_u$ in addition depends on the solar zenith angle ($u = \cos\theta$), and $\mathrm{d}\alpha_\tau$ on the cloud optical thickness τ:

$$\mathrm{d}\alpha_u = 0.53\alpha_S(1-\alpha_S)(1-0.64x-(1-x)u)^{1.2}, \tag{5}$$

$$\mathrm{d}\alpha_\tau = \frac{0.1\tau(\alpha_S + \mathrm{d}\alpha_c)^{1.3}}{(1+1.5\tau)^{\alpha_S}}, \tag{6}$$

where $x = \min\left(\frac{\sqrt{\tau}}{3u}, 1\right)$. The base albedo depends on the snow grain size r_e (in m):

$$\alpha_S = 1.48 - 1.27048 r_e^{0.07}, \tag{7}$$

in which the snow grain size r_e on time step t is parameterised as

$$r_e(t) = \left[r_e(t-1) + \mathrm{d}r_{e,dry} + \mathrm{d}r_{e,wet}\right] f_o + r_{e,0} f_n + r_{e,r} f_r. \tag{8}$$

Here, $\mathrm{d}r_{e,dry}$ and $\mathrm{d}r_{e,wet}$ describe the metamorphism of dry and wet snow respectively, f_o, f_n and f_r are the fractions of old, new and refrozen snow, and $r_{e,0}$ and $r_{e,r}$ are the grain sizes of new and refrozen snow. Dry snow metamorphism is parameterised following Kuipers Munneke et al. (2011b)

$$\frac{\mathrm{d}r_{e,dry}}{\mathrm{d}t} = \left(\frac{\mathrm{d}r_e}{\mathrm{d}t}\right)_0 \left(\frac{\eta}{(r_e - r_{e,0}) + \eta}\right)^{1/\kappa}, \tag{9}$$

where $r_{e,0}$ is the new snow grain size, and the coefficients $\left(\frac{\mathrm{d}r_e}{\mathrm{d}t}\right)_0$, η and κ are obtained from a look-up table. This look-up table is compiled based on simulations with the SNICAR model (Flanner and Zender, 2006), which calculates the snow metamorphism resulting from temperature gradient metamorphism. $\mathrm{d}r_{e,wet}$ is a function of the snow grain size r_e itself and the liquid water content f_{liq} (Brun et al., 1989):

$$\frac{\mathrm{d}r_{e,wet}}{\mathrm{d}t} = \frac{C f_{liq}^3}{4\pi r_e^2}, \tag{10}$$

where C is a constant ($4.22 \cdot 10^{-13}\,\mathrm{m}^3\,\mathrm{s}^{-1}$).

The fractions f_o, f_n and f_r are derived from the snow/firn model, and the grain sizes of new and refrozen snow are constants; the method for determining their values from a tuning exercise is described in Sect. 4.1.

To determine cloud optical thickness τ, an empirical relation between τ and the longwave-equivalent cloud cover N_ϵ is used following Kuipers Munneke et al. (2011a):

$$\tau = c_1 \left(\exp(c_2 N_\epsilon) - 1\right), \tag{11}$$

with fitting parameters c_1 and c_2. N_ϵ is determined using a method described by Kuipers Munneke et al. (2011a) which relates hourly values of downward longwave radiation $LW\downarrow$ to near-surface air temperature T_{2m} as illustrated in Fig. 2a. Red lines indicate quadratic fits through the upper and lower 5 percentile of the data, assuming to represent fully cloudy and clear conditions, respectively. N_ϵ is obtained by linearly interpolating between these upper and lower bounds, yielding values between 0 and 1. Hourly values for cloud cover are then used to obtain values for τ (Fig. 2b). The values used for the fit parameters $c_1 = 5.404$ and $c_2 = 2.207$ (both dimensionless) differ somewhat from Kuipers Munneke et al. (2011a), who used daily values for the fit.

2.3 Observational data

The SEB model is forced with data from the meteorological observatory at the German research station Neumayer, situated on the Ekström ice shelf (König-Langlo, 2017). The observatory has been operational since 1981, and was relocated in 1992 and 2009. In 2016, its location was 70°40'S, 8°16'W (Fig. 1). The observatory is one of only four Antarctic stations –and the only one situated on an ice shelf– that is part of the Baseline Surface Radiation Network (BSRN), a global network of stations with high-quality (artificially ventilated) radiation observations, coordinated by the Alfred Wegener Institute (AWI). We use hourly averages of 2 m temperature (T_{2m}) and specific humidity (q_{2m}), 10 m wind speed (V_{10m}), surface pressure (p) and radiation fluxes for the period April 1992–January 2016 (24 years) to force the SEB model; their uncertainty ranges are

provided in Table 1. Approximately 4.1 % of the data points contained at least one missing variable, which mostly come from daily performed visual inspection of the data. To obtain a continuous data set, all missing data were replaced: pressure, relative humidity, wind speed, temperature and longwave radiation were simply linearly interpolated. In case of shortwave radiation, the missing value was replaced by imitating the average daily cycle of the two preceding days. As the measurement station is visited and maintained every day, the impact of rime formation is limited, as is the tilt of the observation mast, resulting in a high-quality meteorological data set.

Accumulation observations are only available from stake measurements, provided by AWI, which were performed weekly for the period April 1992–January 2009. As timing of precipitation is important for correctly simulating the effects of new snow on snow albedo, we combined the stake observations with precipitation predicted by the regional atmospheric climate model RACMO2.3p2 (Van Wessem et al., 2018) to obtain realistic timing of precipitation in between stake observations, as well as for the post-2009 period. The amount of precipitation modelled by RACMO2 was scaled such that the modelled surface height changes agree with stake measurements; this required a 15.3 % upward adjustment of the modelled precipitation flux.

2.3.1 Local near-surface climate

Neumayer station is located on an ice shelf ∼20 km from Halvfarryggen ice rise to the southeast, ∼100 km from the ice shelf break (grounding line) to the south, ∼20 km from open water/sea ice to the north and ∼5 km to open water/sea ice to the east. As a result, Neumayer experiences relatively mild conditions without significant impact from katabatic winds but with a pronounced influence of synoptic low-pressure systems passing mainly from west to east in the south Atlantic Ocean to the north of the station. The seasonal cycles of 2 m temperature, 10 m wind and 2 m specific humidity are presented in Fig. 3a. Summer temperatures around -4°C and winter temperatures around -25°C imply a substantial (>20 K) seasonal temperature amplitude based on monthly mean values. This is in line with the formation of a surface-based temperature inversion in winter, a phenomenon that is representative for the flat ice shelves as well as the interior ice domes and in contrast to the topographically steeper escarpment zone, where the quasi-continuous mixing by katabatic flow limits the formation of such an inversion (Van den Broeke, 1998). As expected from the strong link to the air temperature through the Clausius-Clapeyron relation and a high annual mean relative humidity of 82 % (relative to either water or ice, depending on the air temperature) because of the proximity of a saturated snow surface and the ocean, the seasonal cycle of q_{2m} closely follows that of temperature.

3 Results: surface energy balance and melt

3.1 SEB model performance and uncertainties

There are several SEB model parameters for which the exact values or formulations are unknown, e.g. the surface roughness length for momentum $z_{0,m}$, the density of new snow ρ_s, the stability functions (required to calculate the turbulent scales) and the effective conductivity, which couples the magnitude of Q_G to the temperature gradient in the snow. We estimated the impact of observational and model uncertainties on modelled melt by running the model 600 times while randomly varying all

hourly observations within the specified measurement uncertainty ranges (Table 1) and using multiple expressions for the heat conductivity and stability functions. Model performance is quantified by comparing modelled with observed T_s and assessing the changes in 24-year total cumulative melt. Note that in this section, the albedo based on observations is used to obtain SW_{net}.

The choice of expressions for the stability functions and heat conductivity did not significantly impact the modelled amount of melt (total within 30 mm w.e. or 2.7 %, not shown). The model outcomes are more sensitive to the choice of surface roughness length for momentum $z_{0,m}$ and the lower limit of density of new snow $\rho_{s,0}$: when $z_{0,m}$ is varied between 0.5 mm and 50 mm and $\rho_{s,0}$ between 150 and 500 kg m^{-3}, the cumulative amount of surface melt over the 24-year period varies between 900–1220 mm w.e., with higher melt values for smaller values of $z_{0,m}$ and $\rho_{s,0}$. Optimal values in terms of simulated T_s are $z_{0,m} = 1.65\,\mathrm{mm}$ and $\rho_{s,0} = 280\,\mathrm{kg\,m^{-3}}$, resulting in a T_s bias of 0.01 K and an RMSD of 0.79 K (Fig. 4). We use these values in the remainder of this study. Figure 5a and b show modelled 24-year cumulative melt and annual melt (Mar–Feb) at Neumayer, combined with uncertainties associated with model parameters. The annual mean values for year X are obtained by averaging monthly values for March of year X until February of year $X+1$. The total melt amounts to 1154 mm w.e., with a small uncertainty associated with measurement uncertainties ($1\sigma \approx 3\,\mathrm{mm}$ w.e., i.e. 0.3 %). The adopted method to estimate this uncertainty has its limitations, as measurement errors are probably autocorrelated: if a measurement at one time is disturbed in some way, it is probably disturbed in a similar way at the next time step. Therefore, this result could be interpreted as a lower bound of the uncertainty range, which is supported by the larger uncertainty estimates (∼15 %) by Van den Broeke et al. (2010), who applied a constant systematic error which can be interpreted as an upper bound on the modelled uncertainty range. This also explains why the uncertainties deriving from the choice of $z_{0,m}$ are so much larger: these runs represent prescribing a systematic error between the true (unknown) value and the chosen value, assuming the true value to be constant, which likely is an oversimplification (Smeets and Van den Broeke, 2008).

The sensitivity to $z_{0,m}$ is somewhat unexpected; following Eq. (3) both $z_{0,h}$ and $z_{0,q}$ decrease for increasing, which acts to dampen the effect on the magnitude of the turbulent fluxes. Our interpretation of this result is that decreasing $z_{0,m}$ and $\rho_{s,0}$ decreases the turbulent fluxes as well as Q_G, reducing the efficiency with which heat is removed from the surface, allowing more energy to be invested in melt. The obtained value for $z_{0,m} = 1.65\,\mathrm{mm}$ is high compared to the average value of $z_{0,m} = 0.1\,\mathrm{mm}$ found during a field campaign at Neumayer in 1982 (König, 1985) but it is not uncommon for snow surfaces (Amory et al., 2017). Measured values of T_s in excess of the melting point in Fig. 4 only occurred in the first 6 seasons; from 1998–99 onwards they were removed by additional post-processing. These measurements mainly reflect uncertainties in the adopted unit value of longwave emissivity and in measured $LW\uparrow$, e.g. from sensor window heating (Smeets et al., 2018) and the fact that the downward facing radiation sensor also measures longwave radiation emitted by the relatively warm air between the surface and the sensor.

3.2 Surface energy balance

Annual (Mar–Feb) mean values of near-surface meteorological quantities and SEB components are presented in Table 2, with seasonal cycles of SEB components presented in Fig. 3b. These show that the summertime SEB is dominated by the radiation

fluxes; despite the high albedo of the snow surface, SW_{net} is the dominant heat source for the skin layer, whereas LW_{net} extracts energy from the surface, most efficiently so in summer when the surface is heated by the sun. In summer, Q_L becomes a significant heat loss in the SEB (sublimation), preventing strong negative Q_S (convection). The seasonal cycle of Q_G is small, indicating a small net transport of heat away from the surface in summer and towards the surface in winter. The net annually integrated amount is less than zero as a result of the refreezing of meltwater, warming the subsurface snow layers.

Significant and previously unreported trends (not shown) are detected in $LW\uparrow$ ($-0.28 \pm 0.14\,\mathrm{W\,m^{-2}\,yr^{-1}}$) and Q_S ($+0.21 \pm 0.07\,\mathrm{W\,m}$ ~~both a result of wintertime trend~~s. $LW\uparrow$ is linked directly to T_s, which shows an insignificant negative trend ($-0.029 \pm 0.026\,\mathrm{K\,yr^{-1}}$), which in magnitude exceeds the negative trend in T_{2m} ($-0.0045 \pm 0.02\,\mathrm{K\,yr^{-1}}$, the probability that the negative trend in T_s is greater in magnitude than the trend in T_{2m} is 0.76). As a result, the temperature gradient near the surface has increased, enhancing Q_S. The negative trend in T_s originates from a decrease in $LW\downarrow$ ($-0.26 \pm 0.17\,\mathrm{W\,m^{-2}\,yr^{-1}}$), which is in turn driven by a slight decrease in cloud cover ($-0.003 \pm 0.001\,\mathrm{yr^{-1}}$). This is suggested independently by the decrease in average winter humidity ($-0.004 \pm 0.002\,\mathrm{g\,kg^{-1}\,yr^{-1}}$). These findings agree with Herman et al. (2013) and Kuipers Munneke et al. (2011a), who determined from satellite observations that summer cloud cover has decreased over that part of coastal Antarctica in the period 1979–2011.

3.3 Melt season

Melt occurs at Neumayer from November until February (Fig. 6), but is highly variable from year to year. The mean annual amount of melt is 50 mm w.e. with an interannual variability of 42 mm w.e. and a range of 2 mm w.e. in 1999–2000 to 176 mm w.e. in 2012–13. Most melt occurs in December and January and the surface only sporadically reaches the melting point in February. Only in 2007 did melt occur in November, and no melt occurs outside these four months. The cumulative melt occurring at Neumayer shows step-wise increases (Fig. 5a), which represent the peaked melt seasons, in which melt occurs on average on 18±10 days. The uncertainty in the number of melt days due to the chosen values of $z_{0,m}$ and $\rho_{s,0}$ is relatively small compared to the interannual variability in melt totals (Fig. 6), implying that this choice does not significantly affect the modelled melt duration, but it does affect the total melt.

To investigate the link between melt and climate, we compare the two summers with the highest (2003–04 and 2012–13, on average 145 mm w.e.) and lowest (1999–2000 and 2014–15, on average 4 mm w.e.) melt amounts. Figure 7 shows the meteorological and SEB components for these years, averaged over December and January. The largest differences are found in T_{2m} (+2.3 K) and SW_{net} (+17 W m^{-2}); based on the measurement uncertainties (Table 1), these differences are significant. In cold summers, the low T_{2m} corresponds to a stronger temperature inversion ($T_{2m} - T_s$), more longwave cooling, less sublimation and a larger Q_S. $SW\downarrow$ and $LW\downarrow$ show almost no difference between high and low melt seasons; therefore, the difference in SW_{net} cannot be caused by a change in cloud cover and is likely caused solely by surface albedo, which suggests an important role for the snowmelt-albedo feedback. This will be elaborated upon in the next section. Finally, the direction of Q_G is reversed; in high melt years, the surface is warmed from below while in low melt years the surface loses heat to the subsurface. More refreezing of meltwater in high melt years warms the near surface snow layers, which in turn leads to a conductive heat flux towards the surface.

Using the subsurface radiation model of Kuipers Munneke et al. (2009), the influence of subsurface penetration of shortwave radiation is estimated. Its inclusion increases the cumulative amount of melt by 13 %, from 1154 mm w.e. to 1326 mm w.e. The absorbed shortwave radiation heats the subsurface layers, but the heat cannot be transported away as effectively as would happen at the surface by turbulent fluxes and longwave radiation. This leads to an increase in total melt.

The findings presented in this section are in good agreement with Van den Broeke et al. (2010), who used a similar approach to calculate the SEB at Neumayer, but used a lower value for $z_{0,m} = 0.32\,\mathrm{mm}$ and a higher snow density that was assumed constant with depth (420 kg m^{-3} cf. 320 kg m^{-3}). Compared to melt estimates from Larsen C ice shelf, obtained through a similar modelling approach by Kuipers Munneke et al. (2012), melt at Neumayer is weak. Owing to its more northerly location, on Larsen C ice shelf an annual (2009–2011) average melt energy of 2.8 W m^{-2} is obtained, compared to the 2009–2011 annual average of 0.7 W m^{-2} obtained at Neumayer; furthermore, in November and February melt occurs much more frequently on Larsen C ice shelf.

4 Results: the snowmelt-albedo feedback

The snowmelt-albedo feedback is a well-known phenomenon, but has not before been quantified for Antarctica. The feedback occurs after the rapid growth of snow grains when meltwater penetrates into the subsurface and refreezes. Because a photon on average travels farther through snow with large particles than in new snow with smaller particles, the probability of it being absorbed is increased, effectively lowering the surface albedo (Gardner and Sharp, 2010). Even without melt, albedo decreases when snow ages, following grain growth from dry snow metamorphism, but this is a much slower process which mainly depends on temperature gradients in the snow, favouring moisture transport onto larger grains. Precipitation of new, fine-grained snow has been shown to inhibit the albedo decrease by metamorphism on the Antarctic plateau (Picard et al., 2012).

To quantify the snowmelt-albedo feedback at Neumayer, we need to be able to switch on and off the albedo dependency on melt-driven grain growth. To that end, we implemented an albedo parameterisation in the SEB model, as described in Sect. 2.2. Because no data on grain size are available from Neumayer, we optimised the albedo model performance by maximising the correspondence between 1) modelled and observed hourly $SW\uparrow$, and 2) the total melt obtained from the calculations based on observed albedo (Sect. 4.1). We compare $SW\uparrow$ instead of the albedo itself because by doing so the hourly values are naturally weighted with its contribution to S_{net} and hence its importance for the SEB. We then perform several runs with different processes switched on and off affecting the surface albedo to investigate the importance of the snowmelt-albedo feedback for melt at Neumayer (Sect. 4.2).

4.1 Optimising the albedo parameterisation

The albedo parameterisation, and especially the expression for snow grain size (Eq. (8)) contains several parameters that are not well constrained, such as new snow grain size $r_{e,0}$ and refrozen snow grain size $r_{e,r}$. These parameters were varied within reasonable ranges to optimise the results: new snow grain size between 0.04 mm and 0.3 mm, refrozen snow grain size between

0.1 mm and 10 mm. The best comparison with observed albedo was achieved when using the look-up table for dry snow metamorphism $\mathrm{d}r_{e,dry}$ corresponding to a grain size of 0.055 mm.

The first step in optimising the parameterisation was to split the summer season into two parts, the 'dry' and the 'wet' season. The respective starts of the dry and wet seasons are the first day on which the sun rises more than 15° above the horizon and the first day that surface melt occurs. The wet season ends when the sun no longer rises higher than 15°. For the dry season, we varied the dry snow metamorphism factor and the new snow grain size to best match observed $SW\uparrow$. This resulted in a new snow grain size of 0.25 mm. This value is then used in the second step, in which the refrozen snow grain size $r_{e,r}$ is varied to best match the cumulative melt using observed albedo. This was achieved for a refrozen snow grain size of 1.45 mm.

This value for refrozen snow grain size is compatible with the typical largest grains in dry metamorphosed snow of O(1 mm), and which Kuipers Munneke et al. (2011b) used as a lower limit for refrozen snow grains. Libois et al. (2015) and Picard et al. (2016) present observations of snow grain sizes on the Antarctic plateau during field campaigns in 2012–13 and 2013–14 as well as estimates from satellite observations. On the plateau, summer temperatures are comparable to Neumayer winter temperatures. Libois et al. (2015) report summertime snow grain size estimates of approximately 0.11 mm (Fig. 6 in their study, reported as a specific surface area $\mathrm{SSA} = \frac{3}{\rho_i r_e}$, where ρ_i is the density of ice and r_e is the snow grain size). In our study, wintertime snow grain sizes approach 0.21 mm. The difference is expected as the plateau is generally much colder than Neumayer. The seasonal cycle of modelled average snow grain size in the upper 7 cm (Fig. 8) is comparable to the one presented in Libois et al. (2015).

When the adopted albedo values are combined with the observations of $SW\uparrow$, the model adequately reproduces the incoming shortwave radiation (Fig. 9, bias = +0.93 W m^{-2}, RMSD = 7.3 W m^{-2}), providing confidence in the modelled albedo.

4.2 Magnitude of the snowmelt-albedo feedback

Three experiments with the SEB model were carried out in addition to the original run (R_0) which uses the measured albedo:

- R_1: the average measured albedo (0.84, determined by adding all $SW\downarrow$ and $SW\uparrow$ for all measurements when the Sun is higher than 15° above the horizon and taking the ratio between the two) is prescribed for the entire period;
- R_2: the full albedo parameterisation is used;
- R_3: refrozen snow does not contribute to the changing snow characteristics, i.e. $f_r = 0$ in Eq. (8).

Figure 10a and b show time series of cumulative and seasonal surface melt for the four experiments. Experiment R_1 underpredicts melt in most seasons, yielding a mean annual amount of surface melt of $39 \pm 27\,\mathrm{mm\,w.e.\,yr^{-1}}$ (c.f. $50 \pm 42\,\mathrm{mm\,w.e.\,yr^{-1}}$ for experiment R_0). More melt was modelled in the 1995–96 melt season, which was characterised by frequent precipitation events and cloudy conditions, keeping observed albedo higher than the long-term mean. The experiment using the full albedo parameterisation (R_2) adequately reproduces the amount of seasonal melt ($50 \pm 34\,\mathrm{mm\,w.e.\,yr^{-1}}$), although melt in e.g. the 2012 melt season is underestimated. Run R_3 represents the situation in which the snowmelt-albedo feedback has been switched off, leading to significantly underpredicted melt ($21 \pm 16\,\mathrm{mm\,w.e.\,yr^{-1}}$).

Defining the strength of the snowmelt-albedo feedback (SMAF) as the ratio between the total seasonal surface melt in experiments R_2 and R_3, we obtain an average value of 2.6, with a range of 1.3 (1996–97) to 4.8 (1993–94, see Fig. 10c). The effect of subsurface penetration of shortwave radiation on this result is estimated by repeating the above experiments with inclusion of the radiation penetration model of Kuipers Munneke et al. (2009). This yielded an average SMAF of 2.3, ranging from 1.5 (2005–06) to 3.2 (2002–03). The main difference between the two experiments is the reduced interannual variability: including penetration of shortwave radiation does not yield SMAF values larger than 3.5. Shortwave radiation penetration heats the subsurface, causing subsurface melt which is less affected by the snowmelt-albedo feedback because the radiative flux is smaller in the subsurface. Therefore, the 'extreme' years in the sense of SMAF are less distinct in the experiment with shortwave radiation penetration. The effect of shortwave radiation penetration is included in the uncertainties indicated in Fig. 10c. Combining this with the uncertainties in observed $SW\uparrow$ and the determination of τ (Fig. 2b) leads to uncertainties in the determination of the SMAF of typically 15 %, with a range of 4 % (1995–96) to 32 % (1993–94).

A weak positive correlation was found between SMAF and $SW\downarrow$ ($R^2 = 0.15,\ p = 0.07$); if $SW\downarrow$ increases, more energy is available at the surface for melting, which is then in turn further intensified by SMAF. Another weak negative correlation was found between SMAF and summer precipitation ($R^2 = 0.13,\ p = 0.09$); snowfall inhibits SMAF as it effectively 'resets' the surface albedo as was also shown by Picard et al. (2012). Alternatively, SMAF could be defined as the ratio between R_0 and R_3, or the ratio between R_0 and R_1', where R_1' uses the average albedo at the end of the winter. Using the former definition, the results become more prone to noise due to the performance of the albedo parameterisation itself. The latter definition neglects the dependency on solar zenith angle and the impact of precipitation. Therefore, we believe defining SMAF as the ratio between R_2 and R_3 is more consistent.

Only few studies report on the snowmelt-albedo feedback concerning the darkening of snow rather than disappearance of it. Box et al. (2012) provide relationships between anomalies of seasonal T_{2m} and SW_{net} (Fig. 5 and 12 of Box et al. (2012)). They find a negative relationship for accumulation regions, i.e. lower 2 m temperatures are associated with smaller SW_{net}. No such relationship is found for Neumayer (not shown).

5 Conclusions

In this study, we used 24 years of high-quality meteorological and radiation observations from the BSRN station Neumayer, situated on Ekström ice shelf, East Antarctica, to force a surface energy balance model. The primary goal was to calculate the amount of melt at Neumayer and to investigate the importance of the snowmelt-albedo feedback. Model performance was evaluated based on the difference between modelled and measured surface temperature, and the calculated melt was tested for measurement and model parameter uncertainties. We found that measurement uncertainties, when considered random in time, do not significantly impact modelled melt at Neumayer (<0.5 % difference). However, melt amount and model performance are sensitive to the values chosen for the surface roughness length for momentum $z_{0,m}$ and lower limit of new snow density $\rho_{s,0}$, thus accurate measurements of these values would further improve future modelling studies. Our results confirm that melt at Neumayer is an intermittent process, occurring on average on only 18 days each summer, totalling 50 mm w.e. and

with an interannual variability of 42 mm w.e. Melt occurs mainly in December and January, sporadically in February and only once melt was modelled in November. Significant and previously unreported trends were found in the net longwave radiation (decreasing) and the sensible heat flux (increasing), but these are unrelated to the melt at Neumayer as they mainly occur in winter and are attributed to a decrease in cloud cover.

The main difference between high and low melt years was found to be surface albedo, implying an important role for the snowmelt-albedo feedback (SMAF). We quantified SMAF by implementing and tuning an albedo parameterisation in the SEB model, which includes the effects of snowfall and wet and dry snow metamorphism on albedo. The albedo parameterisation adequately reproduces the seasonal variability in snow grain size, compared to measurements on the Antarctic Plateau (Libois et al., 2015). Our derived wintertime snow grain sizes at Neumayer are somewhat smaller than the satellite-derived summertime snow grain sizes at the Antarctic Plateau (Libois et al., 2015) owing to the lower temperatures on the plateau. Our main finding is that SMAF on average enhances surface melt at Neumayer by a factor of 2.6 ± 0.8.

Weak correlations were found of SMAF with summertime $SW\downarrow$ and precipitation ($0.1 < R^2 < 0.2$). To assess how the importance of the snowmelt-albedo feedback varies spatially and temporally, the next step in this research will be applying this method to other sites in Antarctica and a regional climate model (Van Wessem et al., 2018).

Code and data availability. The Neumayer data are available upon request via the website of AWI (https://bsrn.awi.de/data/data-retrieval-via-pangaea/). The model output is available upon request by the authors.

Author contributions. CLJ performed the study and wrote the manuscript. PKM assisted with the implementation of the albedo parameterisation. GKL was in charge of the Neumayer data. CHR, PKM, GKL and MRvdB have commented on the manuscript,

Competing interests. The authors declare no competing interests.

Acknowledgements. We would like to thank the AWI for maintaining the station and the Baseline Surface Radiation Network (BSRN) for providing the data, with special thanks to Amelie Driemel for creating a citation reference and Holger Schmithüsen for helping to interpret the data. C.L. Jakobs and C.H. Reijmer acknowledge support from the Netherlands Polar Programme under project number 866.15.204. M.R. van den Broeke acknowledges support from the Netherlands Earth System Science Centre (NESSC). We would like to thank Ghislain Picard and one anonymous referee for their constructive comments.

References

Amory, C., Gallée, H., Naaim-Bouvet, F., Favier, V., Vignon, E., Picard, G., Trouvilliez, A., Piard, L., Genthon, C., and Bellot, H.: Seasonal Variations in Drag Coefficient over a Sastrugi-Covered Snowfield in Coastal East Antarctica, Boundary-Layer Meteorology, 164, 107–133, https://doi.org/10.1007/s10546-017-0242-5, 2017.

Andreas, E. L.: A theory for the scalar roughness and the scalar transfer coefficients over snow and sea ice, Boundary-Layer Meteorology, 38, 159–184, https://doi.org/10.1007/BF00121562, 1987.

Bell, R. E., Chu, W., Kingslake, J., Das, I., Tedesco, M., Tinto, K. J., Zappa, C. J., Frezzotti, M., Boghosian, A., and Lee, W. S.: Antarctic ice shelf potentially stabilized by export of meltwater in surface river, Nature, 544, 344–348, https://doi.org/10.1038/nature22048, 2017.

Box, J. E., Fettweis, X., Stroeve, J. C., Tedesco, M., Hall, D. K., and Steffen, K.: Greenland ice sheet albedo feedback: thermodynamics and atmospheric drivers, The Cryosphere, 6, 821–839, https://doi.org/10.5194/tc-6-821-2012, 2012.

Brandt, R. E. and Warren, S. G.: Solar-heating rates and temperature profiles in Antarctic snow and ice, Journal of Glaciology, 39, 99–110, https://doi.org/10.3198/1993JoG39-131-99-110, 1993.

Brun, E., Martin, E., Simon, V., Gendre, C., and Coléou, C.: An Energy and Mass Model of Snow Cover Suitable for Operational Avalanche Forecasting, Journal of Glaciology, 35, 333–342, https://doi.org/10.3189/S0022143000009254, 1989.

DeConto, R. M. and Pollard, D.: Contribution of Antarctica to past and future sea-level rise, Nature, 531, 591–597, https://doi.org/10.1038/nature17145, 2016.

Dyer, A. J.: A review of flux-profile relationships, Boundary-Layer Meteorology, 7, 363–372, https://doi.org/10.1007/BF00240838, 1974.

Flanner, M. G. and Zender, C. S.: Linking snowpack microphysics and albedo evolution, Journal of Geophysical Research, 111, https://doi.org/10.1029/2005JD006834, 2006.

Flanner, M. G., Zender, C. S., Randerson, J. T., and Rasch, P. J.: Present-day climate forcing and response from black carbon in snow, Journal of Geophysical Research, 112, https://doi.org/10.1029/2006JD008003, 2007.

Fretwell, P., Pritchard, H. D., Vaughan, D. G., Bamber, J. L., Barrand, N. E., Bell, R. E., Bianchi, C., Bingham, R. G., Blankenship, D. D., Casassa, G., Catania, G., Callens, D., Conway, H., Cook, A. J., Corr, H. F. J., Damaske, D., Damm, V., Ferraccioli, F., Forsberg, R., Fujita, S., Gim, Y., Gogineni, P., Griggs, J. A., Hindmarsh, R. C. A., Holmlund, P., Holt, J. W., Jacobel, R. W., Jenkins, A., Jokat, W., Jordan, T., King, E. C., Kohler, J., Krabill, W., Riger-Kusk, M., Langley, K. A., Leitchenkov, G., Leuschen, C., Luyendyk, B. P., Matsuoka, K., Mouginot, J., Nitsche, F. O., Nogi, Y., Nost, O. A., Popov, S. V., Rignot, E., Rippin, D. M., Rivera, A., Roberts, J., Ross, N., Siegert, M. J., Smith, A. M., Steinhage, D., Studinger, M., Sun, B., Tinto, B. K., Welch, B. C., Wilson, D., Young, D. A., Xiangbin, C., and Zirizzotti, A.: Bedmap2: improved ice bed, surface and thickness datasets for Antarctica, The Cryosphere, 7, 375–393, https://doi.org/10.5194/tc-7-375-2013, 2013.

Gardner, A. S. and Sharp, M. J.: A review of snow and ice albedo and the development of a new physically based broadband albedo parameterization, Journal of Geophysical Research: Earth Surface, 115, https://doi.org/10.1029/2009JF001444, 2010.

Hall, A.: The Role of Surface Albedo Feedback in Climate, Journal of Climate, 17, 1550–1568, https://doi.org/10.1175/1520-0442(2004)017<1550:TROSAF>2.0.CO;2, 2004.

Herman, J., DeLand, M. T., Huang, L.-K., Labow, G., Larko, D., Lloyd, S. A., Mao, J., Qin, W., and Weaver, C.: A net decrease in the Earth's cloud, aerosol, and surface 340 nm reflectivity during the past 33yr (1979-2011), Atmospheric Chemistry and Physics, 13, 8505–8524, https://doi.org/10.5194/acp-13-8505-2013, 2013.

Hogg, A. E. and Gudmundsson, G. H.: Impacts of the Larsen-C Ice Shelf calving event, Nature Climate Change, 7, 540–542, https://doi.org/10.1038/nclimate3359, 2017.

Holtslag, A. A. M. and De Bruin, H. A. R.: Applied Modeling of the Nighttime Surface Energy Balance over Land, Journal of Applied Meteorology, 27, 689–704, https://doi.org/10.1175/1520-0450(1988)027<0689:AMOTNS>2.0.CO;2, 1988.

Kingslake, J., Ely, J. C., Das, I., and Bell, R. E.: Widespread movement of meltwater onto and across Antarctic ice shelves, Nature, 544, 349–352, https://doi.org/10.1038/nature22049, 2017.

König, G.: Roughness Length of an Antarctic Ice Shelf, Polarforschung, 55, 27–32, https://doi.org/10.2312/polarforschung.55.1.27, 1985.

König-Langlo, G.: Basic and other measurements, and meteorological synoptical observations from Neumayer Station, 1992-04 to 2016-01, reference list of 572 datasets, https://doi.pangaea.de/10.1594/PANGAEA.874984, 2017.

Kuipers Munneke, P., Van den Broeke, M. R., Reijmer, C. H., Helsen, M. M., Boot, W., Schneebeli, M., and Steffen, K.: The role of radiation penetration in the energy budget of the snowpack at Summit, Greenland, The Cryosphere, 3, 155–165, https://doi.org/10.5194/tc-3-155-2009, 2009.

Kuipers Munneke, P., Reijmer, C. H., and Van den Broeke, M. R.: Assessing the retrieval of cloud properties from radiation measurements over snow and ice, International Journal of Climatology, 31, 756–769, https://doi.org/10.1002/joc.2114, 2011a.

Kuipers Munneke, P., Van den Broeke, M. R., Lenaerts, J. T. M., Flanner, M. G., Gardner, A. S., and Van de Berg, W. J.: A new albedo parameterization for use in climate models over the Antarctic ice sheet, Journal of Geophysical Research: Atmospheres, 116, https://doi.org/10.1029/2010JD015113, 2011b.

Kuipers Munneke, P., Van den Broeke, M. R., King, J. C., Gray, T., and Reijmer, C. H.: Near-surface climate and surface energy budget of Larsen C ice shelf, Antarctic Peninsula, The Cryosphere, 6, 353–363, https://doi.org/10.5194/tc-6-353-2012, 2012.

Kuipers Munneke, P., Ligtenberg, S. R. M., Van den Broeke, M. R., and Vaughan, D. G.: Firn air depletion as a precursor of Antarctic ice-shelf collapse, Journal of Glaciology, 60, 205–214, https://doi.org/10.3189/2014JoG13J183, 2014.

Kuipers Munneke, P., Luckman, A. J., Bevan, S. L., Smeets, C. J. P. P., Gilbert, E., Van den Broeke, M. R., Wang, W., Zender, C. S., Hubbard, B., Ashmore, D., Orr, A., King, J. C., and Kulessa, B.: Intense Winter Surface Melt on an Antarctic Ice Shelf, Geophysical Research Letters, 45, https://doi.org/10.1029/2018GL077899, 2018.

Lenaerts, J. T. M., Van den Broeke, M. R., Déry, S. J., Van Meijgaard, E., Van de Berg, W. J., Palm, S. P., and Sanz Rodrigo, J.: Modeling drifting snow in Antarctica with a regional climate model: 1. Methods and model evaluation, Journal of Geophysical Research: Atmospheres, 117, https://doi.org/10.1029/2011JD016145, 2012.

Lenaerts, J. T. M., Lhermitte, S., Drews, R., Ligtenberg, S. R. M., Berger, S., Helm, V., Smeets, C. J. P. P., Van den Broeke, M. R., Van de Berg, W. J., Van Meijgaard, E., Eijkelboom, M., Eisen, O., and Pattyn, F.: Meltwater produced by wind-albedo interaction stored in an East Antarctic ice shelf, Nature Climate Change, 7, 58–62, https://doi.org/10.1038/nclimate3180, 2017.

Libois, Q., Picard, G., Arnaud, L., Dumont, M., Lafaysse, M., Morin, S., and Lefebvre, E.: Summertime evolution of snow specific surface area close to the surface on the Antarctic Plateau, The Cryosphere, 9, 2383–2398, https://doi.org/10.5194/tc-9-2383-2015, 2015.

Ligtenberg, S. R. M., Helsen, M. M., and Van den Broeke, M. R.: An improved semi-empirical model for the densification of Antarctic firn, The Cryosphere, 5, 809–819, https://doi.org/10.5194/tc-5-809-2011, 2011.

Ligtenberg, S. R. M., Kuipers Munneke, P., and Van den Broeke, M. R.: Present and future variations in Antarctic firn air content, The Cryosphere, 8, 1711–1723, https://doi.org/10.5194/tc-8-1711-2014, 2014.

Luckman, A., A., E., Jansen, D., Kulessa, B., Kuipers Munneke, P., King, J. C., and Barrand, N. E.: Surface melt and ponding on Larsen C Ice Shelf and the impact of föhn winds, Antarctic Science, 26, 625–635, https://doi.org/10.1017/S0954102014000339, 2014.

Massom, R. A., Scambos, T. A., Bennetts, L. G., Reid, P. A., Squire, V. A., and Stammerjohn, S. E.: Antarctic ice shelf disintegration triggered by sea ice loss and ocean swell, Nature, 558, 383–389, https://doi.org/10.1038/s41586-018-0212-1, 2018.

Perovich, D. K., Grenfell, T. C., Light, B., and Hobbs, P. V.: Seasonal evolution of the albedo of multiyear Arctic sea ice, Journal of Geophysical Research, 107, https://doi.org/10.1029/2000JC000438, 2002.

Picard, G., Fily, M., and Gallée, H.: Surface melting derived from microwave radiometers: a climatic indicator in Antarctica, Annals of Glaciology, 46, 29–34, https://doi.org/10.3189/172756407782871684, 2007.

Picard, G., Domine, F., Krinner, G., Arnaud, L., and Lefebvre, E.: Inhibition of the positive snow-albedo feedback by precipitation in interior Antarctica, Nature Climate Change, 2, 795–798, https://doi.org/10.1038/nclimate1590, 2012.

Picard, G., Libois, Q., Arnaud, L., Verin, G., and Dumont, M.: Development and calibration of an automatic spectral albedometer to estimate near-surface snow SSA time series, The Cryosphere, 10, 1297–1316, https://doi.org/10.5194/tc-10-1297-2016, 2016.

Qu, X. and Hall, A.: What Controls the Strength of Snow-Albedo Feedback?, Journal of Climate, 20, 3971–3981, https://doi.org/10.1175/JCLI4186.1, 2007.

Reijmer, C. H. and Oerlemans, J.: Temporal and spatial variability of the surface energy balance in Dronning Maud Land, East Antarctica, Journal of Geophysical Research, 107, https://doi.org/10.1029:2000JD000110, 2002.

Reijmer, C. H., Greuell, W., and Oerlemans, J.: The annual cycle of meteorological variables and the surface energy balance on Berkner Island, Antarctica, Annals of Glaciology, 29, 49–54, https://doi.org/10.3189/172756499781821166, 1999.

Rignot, E., Casassa, G., Gogineni, P., Krabill, W., Rivera, A., and Thomas, R.: Accelerated ice discharge from the Antarctic Peninsula following the collapse of Larsen B ice shelf, Geophysical Research Letters, 31, https://doi.org/10.1029/2004GL020697, 2004.

Scambos, T. A., Bohlander, J. A., Shuman, C. A., and Skvarca, P.: Glacier acceleration and thinning after ice shelf collapse in the Larsen B embayment, Antarctica, Geophysical Research Letters, 31, https://doi.org/10.1029/2004GL020670, 2004.

Schlatter, T. W.: The Local Surface Energy Balance and Subsurface Temperature Regime in Antarctica, Journal of Applied Meteorology, 11, 1048–1062, https://doi.org/10.1175/1520-0450(1972)011<1048:TLSEBA>2.0.CO;2, 1972.

Schneider, T. and Jansson, P.: Internal accumulation in firn and its significance for the mass balance of Storglaciären, Sweden, Journal of Glaciology, 50, 25–34, https://doi.org/10.3189/172756504781830277, 2004.

Shepherd, A., Ivins, E. R., Rignot, E., Smith, B., Van den Broeke, M. R., Velicogna, I., Whitehouse, P. L., Briggs, K. H., Joughin, I., Krinner, G., Nowicki, S., Payne, A. J., Scambos, T. A., Schlegel, N., A, G., Agosta, C., Ahlstrøm, A. P., Babonis, G., Barletta, V. R., Blazquez, A., Bonin, J., Csatho, B., Cullather, R. I., Felikson, D., Fettweis, X., Forsberg, R., Gallée, H., Gardner, A. S., Gilbert, L., Groh, A., Gunter, B., Hanna, E., Harig, C., Helm, V., Horvath, A., Horwath, M., Khan, S., Kjeldsen, K. K., Konrad, H., Langen, P., Lecavalier, B., Loomis, B., Luthcke, S. B., McMillan, M., Melini, D., Mernild, S., Mohajerani, Y., Moore, P., Mouginot, J., Moyano, G., Muir, A., Nagler, T., Nield, G., Nilsson, J., Noël, B. P. Y., Otosaka, I., Pattle, M. E., Peltier, W. R., Pie, N., Rietbroek, R., Rott, H., Sandberg Sørensen, L., Sasgen, I., Save, H., Scheuchl, B., Schrama, E. J. O., Schröder, L., Seo, K.-W., Simonsen, S., Slater, T., Spada, G., Sutterly, T. C., Talpe, M., Tarasov, L., Van de Berg, W. J., Van der Wal, W., Van Wessem, J. M., Vishwakarma, B. D., Wiese, D., and Wouters, B.: Mass balance of the Antarctic Ice Sheet from 1992 to 2017, Nature, 558, 219–222, https://doi.org/10.1038/s41586-018-0179-y, 2018.

Smeets, C. J. P. P. and Van den Broeke, M. R.: Temporal and Spatial Variations of the Aerodynamic Roughness Length in the Ablation Zone of the Greenland Ice Sheet, Boundary-Layer Meteorology, 128, 315–338, https://doi.org/10.1007/s10546-008-9291-0, 2008.

Smeets, C. J. P. P., Kuipers Munneke, P., Van As, D., Van den Broeke, M. R., Boot, W., Oerlemans, J., Snellen, H., Reijmer, C. H., and Van de Wal, R. S. W.: The K-transect in west Greenland: Automatic weather station data (1993-2016), Arctic, Antarctic, and Alpine Research, 50, https://doi.org/10.1080/15230430.2017.1420954, 2018.

Tedesco, M.: Assessment and development of snowmelt retrieval algorithms over Antarctica from K-band spaceborn brightness temperature (1979-2008), Remote Sensing of Environment, 113, 979–997, https://doi.org/10.1016/j.rse.2009.01.009, 2009.

Trusel, L. D., Frey, K. E., Das, S. B., Kuipers Munneke, P., and Van den Broeke, M. R.: Satellite-based estimates of Antarctic surface meltwater fluxes, Geophysical Research Letters, 40, 6148–6153, https://doi.org/10.1002/2013GL058138, 2013.

Trusel, L. D., Frey, K. E., Das, S. B., Karnauskas, K. B., Kuipers Munneke, P., Van Meijgaard, E., and Van den Broeke, M. R.: Divergent trajectories of Antarctic surface melt under two twenty-first-century climate scenarios, Nature Geoscience, 8, 927–934, https://doi.org/10.1038/NGEO2563, 2015.

Turner, J., Orr, A., Gudmundsson, G. H., Jenkins, A., Bingham, R. G., Hillenbrand, C.-D., and Bracegirdle, T. J.: Atmosphere-ocean-ice interactions in the Amundsen Sea Embayment, West Antarctica, Reviews of Geophysics, 55, 235–276, https://doi.org/10.1002/2016RG000532, 2017.

Van As, D., Fausto, R. S., Colgan, W. T., Box, J. E., Ahlstrøm, A. P., Andersen, S. B., Andersen, M. L., Charalampidis, C., Citterio, M., Edelvang, K., Jensen, T. S., Larsen, S. H., Machguth, H., Nielsen, S., Veicherts, M., and Weidick, A.: Darkening of the Greenland ice sheet due to the melt-albedo feedback observed at PROMICE weather stations, Geological Survey of Denmark and Greenland Bulletin, 28, 69–72, 2013.

Van den Broeke, M. R.: The semi-annual oscillation and Antarctic climate. Part 1: influence on near surface temperatures (1957-79), Antarctic Science, 10, 175–183, https://doi.org/10.1017/S0954102098000248, 1998.

Van den Broeke, M. R., Reijmer, C. H., and Van de Wal, R. S. W.: Surface radiation balance in Antarctica as measured with automatic weather stations, Journal of Geophysical Research, 109, https://doi.org/10.1029/2003JD004394, 2004.

Van den Broeke, M. R., Reijmer, C. H., Van As, D., Van de Wal, R. S. W., and Oerlemans, J.: Seasonal cycles of Antarctic surface energy balance from automatic weather stations, Annals of Glaciology, 41, 131–139, https://doi.org/10.3189/172756405781813168, 2005.

Van den Broeke, M. R., König-Langlo, G., Picard, G., Kuipers Munneke, P., and Lenaerts, J. T. M.: Surface energy balance, melt and sublimation at Neumayer Station, East Antarctica, Antarctic Science, 22, 87–96, https://doi.org/10.1017/S0954102009990538, 2010.

Van der Veen, C. J.: Fracture propagation as means of rapidly transferring surface meltwater to the base of glaciers, Geophysical Research Letters, 34, https://doi.org/10.1029/2006GL028385, 2007.

Van Wessem, J. M., Van de Berg, W. J., Noël, B. P. Y., Van Meijgaard, E., Birnbaum, G., Jakobs, C. L., Krüger, K., Lenaerts, J. T. M., Lhermitte, S., Ligtenberg, S. R. M., Medley, B., Reijmer, C. H., Van Tricht, K., Trusel, L. D., Van Ulft, L. H., Wouters, B., Wuite, J., and Van den Broeke, M. R.: Modelling the climate and surface mass balance of polar ice sheets using RACMO2, part 2: Antarctica (1979-2016)., The Cryosphere, 12, 1479–1498, https://doi.org/10.5194/tc-2017-202, 2018.

Wiscombe, W. J. and Warren, S. G.: A Model for the Spectral Albedo of Snow. I: Pure Snow, Journal of the Atmospheric Sciences, 37, 2712–2733, https://doi.org/10.1175/1520-0469(1980)037<2712:AMFTSA>2.0.CO;2, 1980.

Wouters, B., Martin-Español, A., Helm, V., Flament, T., Van Wessem, J. M., Ligtenberg, S. R. M., Van den Broeke, M. R., and Bamber, J. L.: Dynamic thinning of glaciers on the Southern Antarctic Peninsula, Science, 348, 899–903, https://doi.org/10.1126/science.aaa5727, 2015.

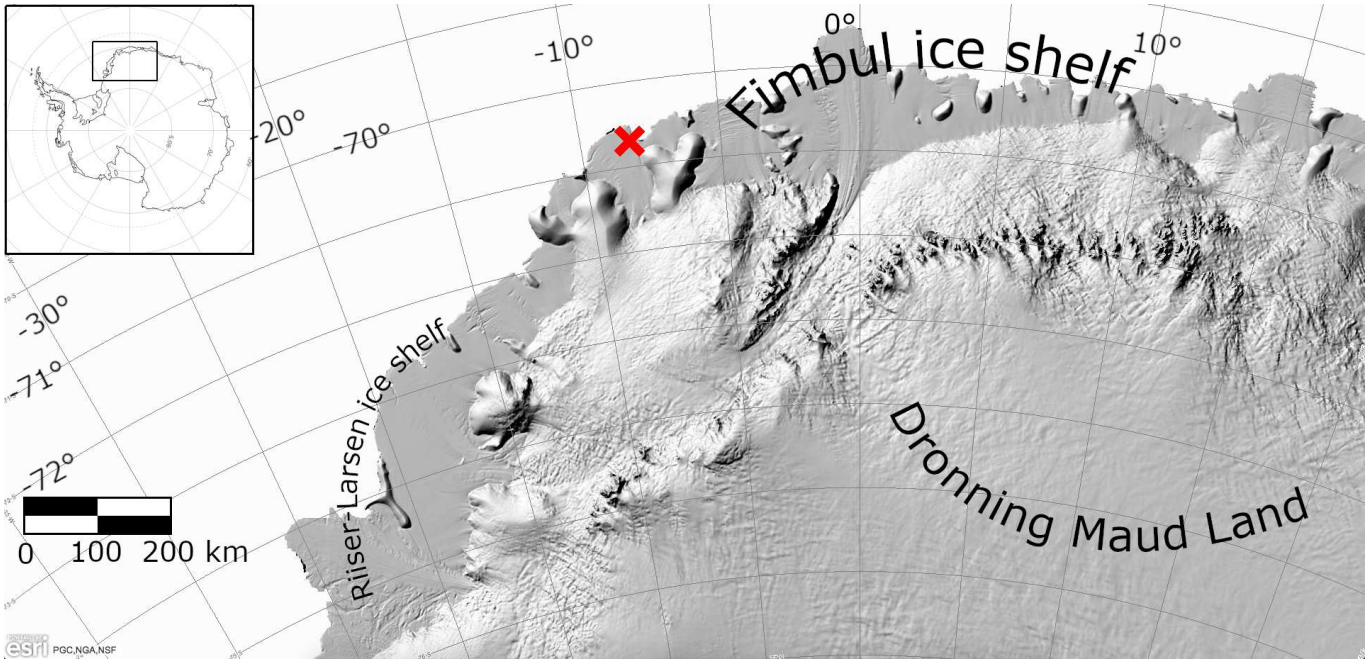

Figure 1. Map of the Antarctic continent, the red cross indicates the location of Neumayer Station. Imagery (C) 2016 DigitalGlobe, Inc.

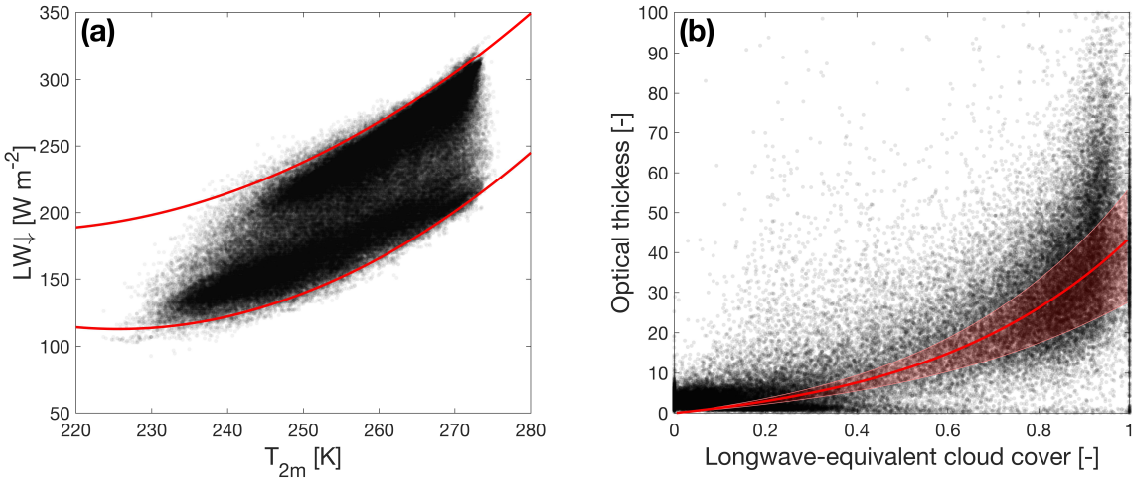

Figure 2. **(a)** Downward longwave radiation versus air temperature. The red lines are quadratic fits of the upper and lower 5 percentile boundaries. The longwave-equivalent cloud cover is determined by linear interpolation between these bounds. **(b)** Optical thickness versus cloud cover. The red line resembles the best fit to a function $\tau = c_1 \left(e^{c_2 N_\epsilon} - 1\right)$, the shaded area indicates the 95% uncertainty range.

Table 1. Listing of used measurement variables and their associated measurement errors.

Variable	Neumayer errors
V_{10m}	max(0.5 m/s, 5%)
$SW\downarrow$	5 W/m^2
$SW\uparrow$	5 W/m^2
$LW\downarrow$	5 W/m^2
$LW\uparrow$	5 W/m^2
T_{2m}	0.1°C
RH_{2m}	5%
p	0.5 hPa

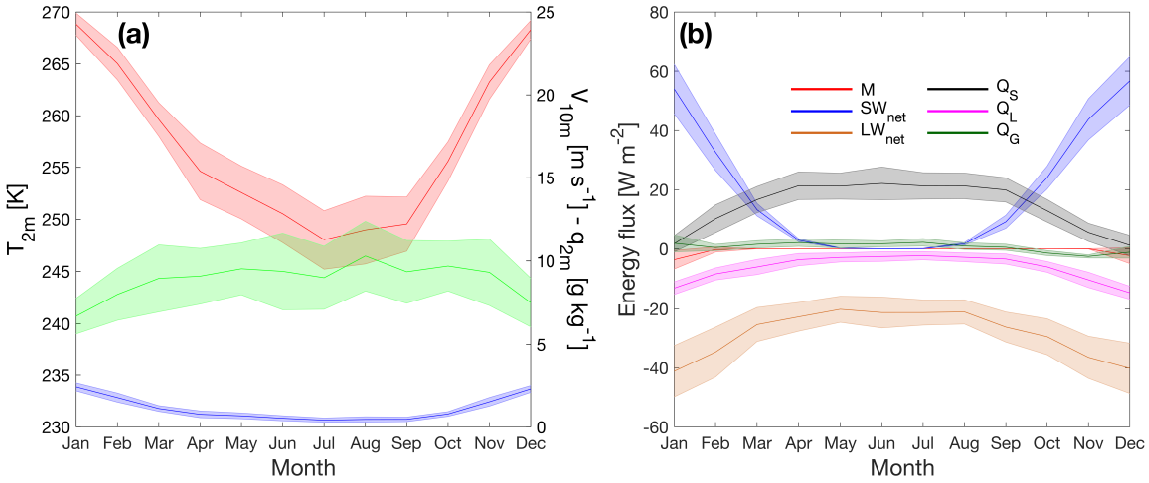

Figure 3. **(a)** Seasonal cycles of 2 m temperature (red, left axis), 10 m wind speed (green, right axis) and 2 m specific humidity (blue, right axis). Shaded areas indicate the standard deviations of monthly means. **(b)** Same as **(a)** for melt (red), net shortwave radiation (blue), net longwave radiation (orange), sensible heat (black), latent heat (magenta) and ground heat (green).

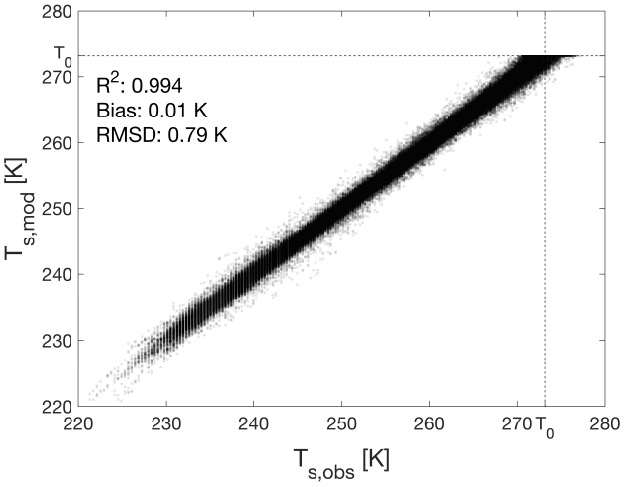

Figure 4. Daily values of modelled versus measured T_s for the parameter settings used in this study: $z_{0,m} = 1.65\,\mathrm{mm}$, $\rho_{s,0} = 280\,\mathrm{kg\,m^{-3}}$.

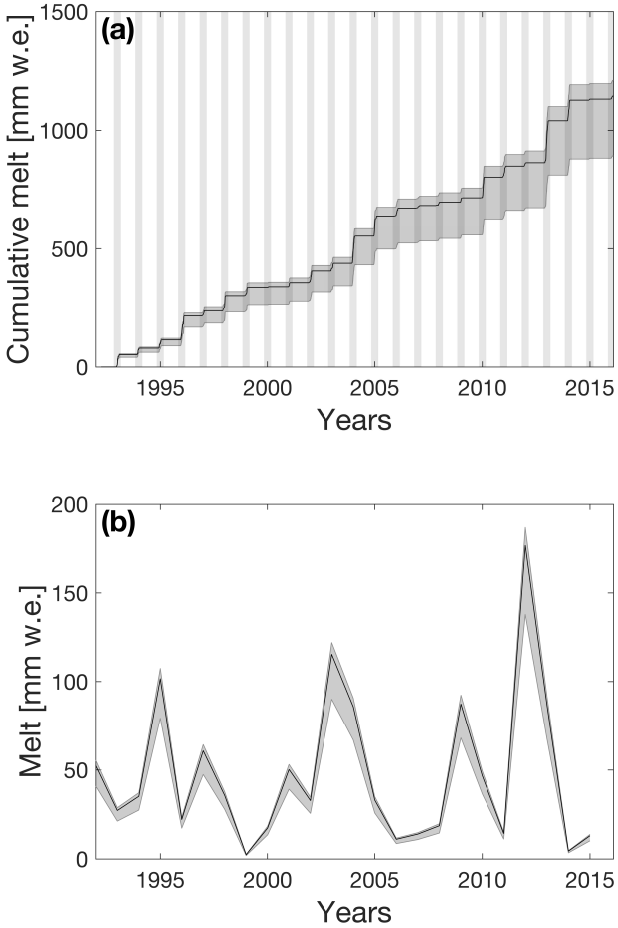

Figure 5. Effect of model uncertainties on **(a)** cumulative melt and **(b)** seasonal melt. The shaded area indicates the 1σ range due to model uncertainties (changing $z_{0,m}$ and $\rho_{s,0}$ between their respective values) which is asymmetrical because the values that are used for the rest of the study ($z_{0,m} = 1.65\,\mathrm{mm}$, $\rho_{s,0} = 280\,\mathrm{kg\,m^{-3}}$) are not in the middle of the range that was probed. The vertical grey patches in **a)** indicate Nov–Feb of each year. Note that **(b)** ends earlier than **(a)** because the observations do not cover the 2015–16 melt season entirely.

Table 2. Mean annual values and interannual variability (calculated as standard deviations of monthly means) of meteorological variables and SEB components. For precipitation and melt, total annual values are given.

Variable	Yearly mean	Variability
T_{2m} (K)	257.1	0.7
T_s (K)	256.0	0.8
q_{2m} (g kg^{-1})	1.1	0.1
V_{10m} (m s^{-1})	8.9	0.6
p (hPa)	981.6	2.0
SW_{net} (W m^{-2})	20	2
$SW\downarrow$ (W m^{-2})	127	3
$SW\uparrow$ (W m^{-2})	107	2
LW_{net} (W m^{-2})	-28	3
$LW\downarrow$ (W m^{-2})	218	5
$LW\uparrow$ (W m^{-2})	246	4
Q_S (W m^{-2})	14.5	2.7
Q_L (W m^{-2})	-6.3	1.2
Q_G (W m^{-2})	0.7	0.4
M (W m^{-2})	0.5	0.4
Precipitation (mm w.e.)	415	86
Melt (mm w.e.)	50	42

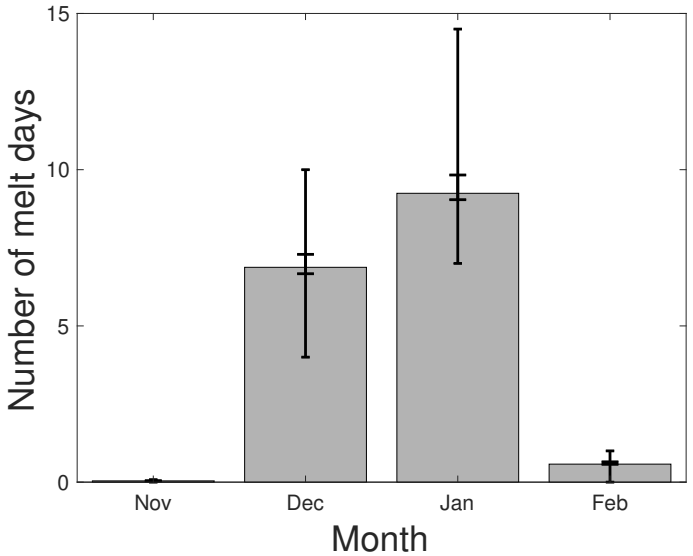

Figure 6. Average number of melt days per month at Neumayer. The inner error bars (with larger caps) indicate the 1σ uncertainty range resulting from the runs performed with different settings for roughness length z_0 and lower limit of new snow density $\rho_{s,0}$ (Sect. 3.1). The outer error bars (with smaller caps) indicate the 1σ range of the interannual variability.

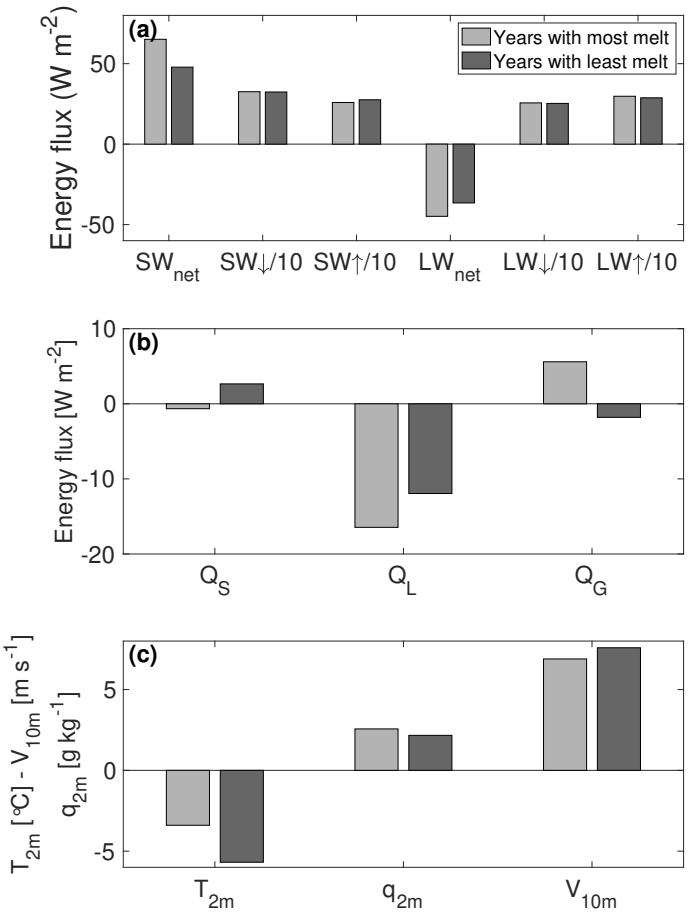

Figure 7. Average values of some SEB components **(a)** and **(b)** and some meteorological variables **(c)** for December and January in the years with the highest (light grey) and lowest (dark grey) amount of melt, as identified in Sect. 3.3. Note that $SW\downarrow$, $SW\uparrow$, $LW\downarrow$ and $LW\uparrow$ are scaled by a factor of 10 in **(a)** for clarification.

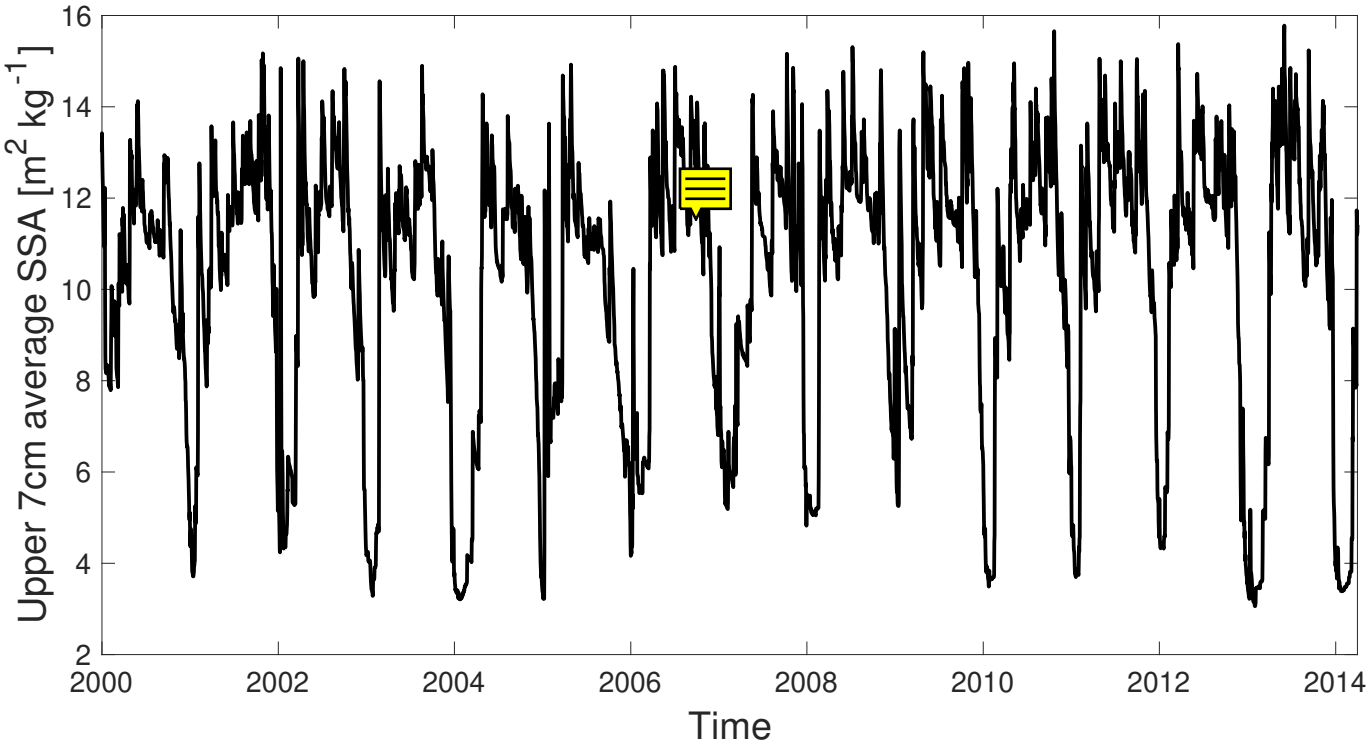

Figure 8. Seasonal cycle of modelled average grain size in the upper 7 cm for the period 2000–2014. The grain size is expressed in terms of specific surface area ($\mathrm{SSA} = \frac{3}{\rho_i r_e}$) rather than grain size itself, to allow for a comparison with Fig. 6 of Libois et al. (2015).

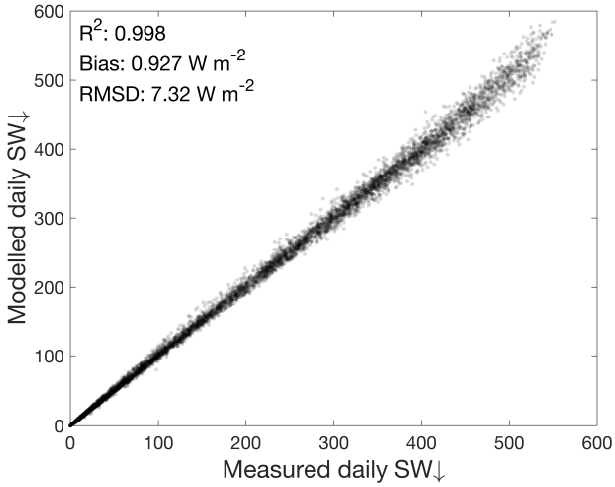

Figure 9. Measured versus modelled daily average incoming shortwave radiation ($SW\downarrow$). The modelled $SW\downarrow$ was obtained by dividing the hourly measured $SW\uparrow$ by the calculated hourly albedo.

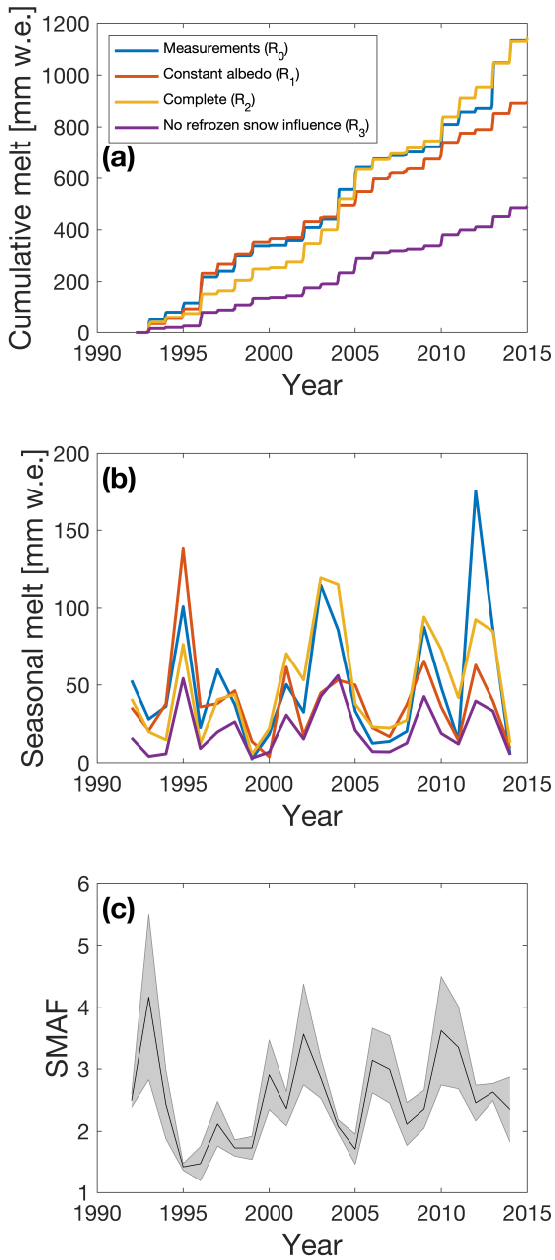

Figure 10. **(a)** Timeseries of cumulative amount of melt for the run with measured albedo (R_0, blue), a constant albedo of 0.84 (R_1, red), a run in which refrozen snow does impact snow grain size (R_2, yellow) and a run in which snow grain size is not influenced by refrozen snow (R_3, purple). **(b)** Same as **(a)** but for seasonal amount of melt. **(c)** Ratio of modelled surface melt between yellow and purple lines in **(a)** and **(b)** (runs R_2 and R_3 respectively). The grey area indicates the uncertainty coming from the uncertainty in the determination of τ (Fig. 2b)), $\pm 5\,\mathrm{W\,m^{-2}}$ measurement uncertainty in $SW\uparrow$ and the inclusion of shortwave radiation penetration.